Test-area simulation method for the direct determination of the interfacial tension of systems with continuous or discontinuous potentials

Guy J. Gloor[a] and George Jackson[b]
Department of Chemical Engineering, Imperial College London, South Kensington Campus, London SW7 2AZ, United Kingdom

Felipe J. Blas and Enrique de Miguel
Departamento de Física Aplicada, Facultad de Ciencias Experimentales, Universidad de Huelva, 21071 Huelva, Spain

(Received 17 June 2005; accepted 25 July 2005; published online 4 October 2005)

A novel test-area (TA) technique for the direct simulation of the interfacial tension of systems interacting through arbitrary intermolecular potentials is presented in this paper. The most commonly used method invokes the mechanical relation for the interfacial tension in terms of the tangential and normal components of the pressure tensor relative to the interface (the relation of Kirkwood and Buff [J. Chem. Phys. **17**, 338 (1949)]). For particles interacting through discontinuous intermolecular potentials (e.g., hard-core fluids) this involves the determination of δ functions which are impractical to evaluate, particularly in the case of nonspherical molecules. By contrast we employ a thermodynamic route to determine the surface tension from a free-energy perturbation due to a test change in the surface area. There are important distinctions between our test-area approach and the computation of a free-energy difference of two (or more) systems with different interfacial areas (the method of Bennett [J. Comput. Phys. **22**, 245 (1976)]), which can also be used to determine the surface tension. In order to demonstrate the adequacy of the method, the surface tension computed from test-area Monte Carlo (TAMC) simulations are compared with the data obtained with other techniques (e.g., mechanical and free-energy differences) for the vapor-liquid interface of Lennard-Jones and square-well fluids; the latter corresponds to a discontinuous potential which is difficult to treat with standard methods. Our thermodynamic test-area approach offers advantages over existing techniques of computational efficiency, ease of implementation, and generality. The TA method can easily be implemented within either Monte Carlo (TAMC) or molecular-dynamics (TAMD) algorithms for different types of interfaces (vapor-liquid, liquid-liquid, fluid-solid, etc.) of pure systems and mixtures consisting of complex polyatomic molecules. © *2005 American Institute of Physics*. [DOI: 10.1063/1.2038827]

I. INTRODUCTION

Interfacial systems are ubiquitous in both nature and our technologically based society. The subsistence of life itself is in a large part due to the lipid bilayer structures that form cell membranes and provide an active interface between the aqueous environments inside and outside the cell; the selectivity of the membrane proteins to the various solutes and other molecular species supports the complex functions of the cell. An understanding of interfaces and inhomogeneous systems is essential to all manner of industrial processes. For example, the surface tension between a liquid and its vapor or two coexisting liquids is of central importance in understanding capillary rise and the solubilization of immiscible fluids. Surface active agents (surfactants) are routinely used as detergents in products ranging from washing powders to toothpaste and lubricants; the water-surfactant interfaces of lyotropic liquid-crystalline amphiphiles are designed to give a formulation (soaps, cosmetics, foodstuffs, etc.) the desired macroscopic properties. At another length scale, colloidal suspensions of large particles are stabilized by tuning the interactions of the colloid surface with the solvent.

It is not therefore surprising that molecular theories of inhomogeneous systems are now well developed,[1–3] with major advances since the pioneering work of van der Waals.[4] Molecular simulation techniques are also routinely used to examine inhomogeneous systems. It is relatively straightforward to simulate the interfacial profile between two coexisting fluids[1] or a fluid in contact with a solid surface,[5] and complex systems including surfactant solutions,[6] biological membranes,[7,8] and nematic liquid-crystalline films,[9–13] and coexisting liquid-crystalline phases which possess orientational and translational order[14] have now been simulated. The interfacial tension is generally more difficult to determine, particularly in the case of large nonspherical or polyatomic molecules or of systems interacting through discontinuous potentials. The essentially exact simulation data for the interfacial properties of fluids and fluid mixtures not only allow one to understand the nature of the interface at the microscopic level, but also provide a basis from which to test

[a]Present address: Schering-Plough Research Institute, 1011 Morris Ave. U18-1,13 Union, New Jersey 07083, USA.
[b]Author to whom correspondence should be addressed. Electronic mail: g.jackson@imperial.ac.uk

 © 2005 American Institute of Physics

Downloaded 10 Oct 2005 to 155.198.160.109. Redistribution subject to AIP license or copyright, see http://jcp.aip.org/jcp/copyright.jsp

the adequacy of a specific intermolecular potential model and the approximations inherent in a given molecular theory.[15] For example, we have recently assessed the adequacy of a density functional based on the statistical associating fluid theory (SAFT) in describing the density profile and vapor-liquid surface tension of associating chain molecules by comparison with simulation.[16]

Three general types of simulation techniques can be used to determine the surface tension γ of fluids. The first, and most widespread, class of technique involves a mechanical route which requires the calculation of the tensorial components of the pressure.[1] In the case of a planar interface (which is assumed to be perpendicular to the z axis of a Cartesian frame of reference) the surface tension is given by

$$\gamma = \int_{-\infty}^{\infty} dz[P_N(z) - P_T(z)], \tag{1}$$

where $P_N(z)=P$ and $P_T(z)$ are the normal and tangential components of the pressure, and P is the equilibrium pressure. The use of the mechanical expression thus involves the computation of the components of the pressure tensor as a function of the distance from the interface. In practice the tensorial components are related to the derivative of the intermolecular potential to give an explicit expression for the interfacial tension, as was first shown by Kirkwood and Buff;[17] the explicit form of the Kirkwood-Buff relation is given in the following section. The second route to the surface tension involves a thermodynamic perspective in which the free-energy difference between two (or more) systems with different interfacial areas is determined to estimate the surface tension (the method of Bennett[18]). The standard thermodynamic relation for the change in the Helmholtz free energy A in terms of changes in the temperature T, volume V, number of particles N_i of each species i, and interfacial area $\mathcal{A}$ is[1]

$$dA = -SdT - PdV + \sum_i \mu_i dN_i + \gamma d\mathcal{A}, \tag{2}$$

where S is the entropy, and μ_i is the chemical potential of component i. At constant temperature, volume, and number of particles, the surface tension can thus be defined as

$$\gamma = \left(\frac{\partial A}{\partial \mathcal{A}}\right)_{N_i,V,T}, \tag{3}$$

i.e., the change in free energy for an infinitesimal change in the interfacial area. One can also integrate the differential relation (2) to identify the surface contribution A^s to the total Helmholtz free energy as the difference $A^s = A - A^\alpha - A^\beta$, where $A = -pV + \Sigma_i \mu_i N_i + \gamma\mathcal{A}$ is the total free energy of the inhomogeneous system with two coexisting phases α and β, and $A^\alpha = -pV^\alpha + \Sigma_i \mu_i N_i^\alpha$ and $A^\beta = -pV^\beta + \Sigma_i \mu_i N_i^\beta$ are the free energies of each homogeneous phase. For a system with two coexisting phases the so-called surface free energy can be defined as

$$A^s = \sum_i \mu_i N_i^s + \gamma\mathcal{A}, \tag{4}$$

where $N_i^s = N_i - N_i^\alpha - N_i^\beta$ represents the surface contribution to the number of particles of each species. Clearly, the surface tension can be identified with the surface free energy per unit area, $\gamma = A^s/\mathcal{A}$, only when the surface contributions $N_i^s = 0$ vanish for all species. The more natural thermodynamic potential when dealing with interfacial systems is the grand potential $\Omega = A - \Sigma_i \mu_i N_i$ for now the surface grand potential Ω^s is always given by

$$\Omega^s = \gamma\mathcal{A}. \tag{5}$$

These thermodynamic expressions can be used to estimate the surface tension from the free-energy difference of systems with and without an interface. The third class of technique is based on the concepts of finite-size scaling. In the case of the method developed by Binder[19] one estimates a Landau free-energy barrier between coexisting phases from a simulation of the density of states, which in the limit of large system sizes can be related to the interfacial tension. Alternatively, a capillary-wave model[1,20] can be used to estimate the interfacial tension from a finite-size analysis of the width of the interfacial profile (or from a Fourier analysis of the amplitude of the capillary waves). There are advantages and disadvantages inherent in the application of the various techniques: the mechanical approach is difficult to apply to systems consisting of molecules which interact through discontinuous potentials or which are nonspherical, and is relatively inefficient; two (or more) simulations have to be performed with the free-energy difference method, something which can be quite computationally demanding; the density-of-states method fails at low temperatures because the high-density configurations are difficult to sample adequately.

In this paper we present a novel test-area Monte Carlo (TAMC) method for the efficient determination of the surface tension from a single simulation. The approach can be applied to molecules interacting through continuous or discontinuous potentials, to highly nonspherical molecules, and to mixtures over a wide range of temperature. In order to demonstrate the validity of the approach we examine the vapor-liquid interface of Lennard-Jones (LJ) systems for different values of the potential cutoff, for which there exists a wealth of simulation data, and of square-well systems of variable range. Comparisons are made with the surface tension determined with the other techniques, and the advantages of the TAMC method are highlighted. Before our TAMC method for the computation of the surface tension is discussed in detail, it is important to place the available techniques in historical context and provide a brief review of the key milestones in simulating interfacial systems.

II. SIMULATION OF THE INTERFACIAL TENSION

As we mentioned earlier, molecular simulation is now commonplace as a technique for studying complex fluids, and can readily be implemented to different types of systems under different conditions (thermodynamic ensembles).[21] The stabilization of a fluid interface (corresponding to a system with a nonuniform density within a single simulation

Downloaded 10 Oct 2005 to 155.198.160.109. Redistribution subject to AIP license or copyright, see http://jcp.aip.org/jcp/copyright.jsp

box) is relatively straightforward with molecular dynamics (MD) or Monte Carlo (MC). This was first demonstrated by Croxton and Ferrier[22] who performed molecular-dynamics simulations of the vapor-liquid interface of a LJ system in two dimensions. Shortly afterwards Leamy *et al.*[23] stabilized the interface of a three-dimensional lattice gas (Ising model) by Monte Carlo simulation. The first estimates of the vapor-liquid surface tension from simulations of LJ systems were made by Lee *et al.*[24] and by Liu[25] using the mechanical relation of Kirkwood and Buff[17] within a standard Metropolis Monte Carlo scheme. A couple of years later a thermodynamic approach based on the free-energy difference method of Bennett[18] was used by Miyazaki *et al.*[26] to determine the surface tension of the LJ system by simulating the free-energy change associated with the creation of an interface from a block of liquid in a series of steps (17 in all). It is rather surprising that though the thermodynamic route can lead to an improved accuracy of the simulated surface tension (in the case of the LJ fluid, Miyazaki *et al.* quote an error which is an order of magnitude smaller than that obtained from the mechanical route), little use of this type of approach has been made since. The alternative approach of Binder,[19] which allows one to estimate the surface tension from a knowledge of the energy barrier between the two coexisting states, is also less widespread than those based on the calculation of the pressure tensor. Molecular dynamics is the technique of choice for the simulation of interfacial systems as the pressure tensor (and surface tension) can be evaluated directly from the forces.

The early simulation studies[22,24,25,27] appeared to suggest that the vapor-liquid interface exhibited marked layering, but this view was later discounted as being due to slow convergence and system-size effects.[28–31] The constraints on computational time meant that the early work was restricted to relatively small systems (ca. $N=200$–300 particles), and as a consequence pronounced finite-size effects were seen. The molecular-dynamics simulations of $N=4080$ LJ particles undertaken by Chapela *et al.*[31] were quite ambitious for the time, and their accurate interfacial data remained the standard for many years. It was not until the work of Chen[32] that a clearer understanding of the finite-size effects involved in the simulation of the vapor-liquid surface tension emerged; Chen[32] showed that a minimum cell dimension of ten molecular diameters ($L>10\sigma$) was required for accurate results. The large systems simulated by Chapela *et al.*[31] exceeded this requirement. The significant discrepancies in the estimates of the vapor-liquid surface tension reported in the numerous simulation studies of LJ fluids cannot, however, all be attributed to finite-size effects. An inconsistent treatment of the long-range interactions in Monte Carlo and molecular dynamics has also led to conflicting results for the interfacial properties,[33] and great care has to be employed when using truncated potentials. The problems associated with the truncation of the potential have been very clearly illustrated by Trokhymchuk and Alejandre[34] by simulating LJ particles for various values of the potential cutoff r_c. A relatively large value of the cutoff ($r_c=5.5\sigma$) has to be used in order to obtain a good estimate of the surface tension of the full LJ potential; for example, the surface tension of the system with the commonly employed cutoff of $r_c=2.5\sigma$ is about half that of the system interacting through the full potential.

With great improvements in computing power since the early 1970s the simulation of interfacial properties for relatively complex systems is now possible; in view of the large body of research in the area we mention only the most relevant work here. Some caution should be taken in assessing the findings reported in these studies as the first simulations of the interfaces of complex molecules (e.g., water[35]) were attempted prior to a full understanding of truncation effects in the simpler LJ system.[34] Molecular-dynamics simulation has now been used to simulate the vapor-liquid interfacial structure and surface tension of water,[35,36] carbon tetrachloride,[37] acetone,[38] pentane,[39] hexane, decane, hexadecane,[40] heptadecane,[41] and eicosane.[42] The liquid-liquid interface of mixtures of immiscible components has also been examined by molecular simulation (see Ref. 43 for a review).

By contrast, however, simulations of the interfacial properties of systems interacting via discontinuous potentials still remain relatively rare. This is because the pressure tensor and surface tension of such systems are more difficult to treat, due to the discontinuous nature of the force (derivative of the potential). To our knowledge the first simulated values of the vapor-liquid surface tension of the confined square-well fluid were reported by Henderson and van Swol[44] using the mechanical relation and a thermodynamic route (square gradient approximation of the free-energy functional). Extra care must be taken in the calculation of the surface tension of such systems when the mechanical route is employed within a Monte Carlo approach (e.g., see Ref. 45). In the case of spherically symmetric potentials such as the square well, impulsive (collision-by-collision) molecular-dynamics simulation offers a significant advantage, but this type of approach is difficult to undertake for systems comprising nonspherical particles. Data for the vapor-liquid surface tension of square-well fluids of variable range obtained using the mechanical route by both Monte Carlo[45,46] and molecular-dynamics[47] simulation have recently been reported. The method of Binder[19] can also be used to determine the surface tension of systems with discontinuous potentials from the density of states obtained during a grand canonical Monte Carlo simulation. Singh *et al.*[47] have coupled the Binder method with an improved sampling (transition matrix Monte Carlo) to determine the surface tension of square-well fluids of range $\lambda/\sigma=1.5$, 1.75, and 2. As we have already mentioned this method is not suitable for use at temperatures well below the critical point (e.g., close to the triple point) due to inefficiencies in sampling the liquid states at low temperatures. A simulation technique which remains efficient over the entire temperature range and avoids the difficulties associated with the mechanical route is therefore particularly desirable. We propose a novel test-area Monte Carlo simulation scheme based on the formal thermodynamic definition of the surface tension which is simple, efficient, and can easily be applied to systems interacting via discontinuous potentials, particularly in the case of more complex polyatomic molecules. In the following sections we will briefly review the microscopic (sta-

Downloaded 10 Oct 2005 to 155.198.160.109. Redistribution subject to AIP license or copyright, see http://jcp.aip.org/jcp/copyright.jsp

tistical mechanical) techniques which are currently employed in simulating the surface tension of fluids, and then present our approach in more detail.

A. Mechanical relation

As we have seen the determination of the surface tension from the mechanical expression [Eq. (1)] requires an evaluation of the components of the pressure tensor in terms of the intermolecular interactions. The pressure tensor is a microscopic function that, in general, varies from point to point in the fluid. It can be defined as the ensemble average of the negative of the stress tensor at position $\mathbf{r}$.[48,49] The stress tensor contains two terms: a kinetic term, arising from the change in momentum due to particles crossing the boundaries of an elemental volume at $\mathbf{r}$, and a configurational term, related to the change in momentum due to external fields and the intermolecular interactions between the particles within the elemental volume and the rest of the particles of the fluid. For a homogeneous fluid the components of the pressure tensor do not depend on $\mathbf{r}$. In the absence of external fields, and assuming pairwise interactions as well as central forces, the tensorial components of a homogeneous system can be defined as

$$\begin{aligned}\bar{P}_{\alpha\beta} &= \rho kT\delta_{\alpha\beta} + \frac{1}{V}\left\langle \sum_i \sum_{j>i} r_{ij}^{\alpha} f_{ij}^{\beta} \right\rangle \\ &= \rho kT\delta_{\alpha\beta} - \frac{1}{V}\left\langle \sum_i \sum_{j>i} r_{ij}^{\alpha} \frac{r_{ij}^{\beta}}{r_{ij}} \frac{du(r_{ij})}{dr_{ij}} \right\rangle, \end{aligned} \tag{6}$$

where $\delta_{\alpha\beta}$ is the Kronecker delta, the brackets denote a configurational average, r_{ij}^{α} is the α component of the intermolecular vector $\mathbf{r}_{ij}$, f_{ij}^{β} is the β component of the intermolecular force $\mathbf{f}_{ij}$, $u(r_{ij})$ is the pair potential, k is the Boltzmann constant, and $\rho = N/V$ is the number density. For a homogeneous fluid the Cartesian components are $\bar{P}_{xx} = \bar{P}_{yy} = \bar{P}_{zz} = P$, where P is the bulk pressure. Alternatively, this can be defined as an average $P = (\bar{P}_{xx} + \bar{P}_{yy} + \bar{P}_{zz})/3$, from which the expression for the bulk pressure can be cast in the familiar virial form,[1,50]

$$\begin{aligned}P &= \rho kT + \frac{1}{3V}\left\langle \sum_i \sum_{j>i} \mathbf{r}_{ij} \cdot \mathbf{f}_{ij} \right\rangle \\ &= \rho kT - \frac{1}{3V}\left\langle \sum_i \sum_{j>i} r_{ij} \frac{du(r_{ij})}{dr_{ij}} \right\rangle. \end{aligned} \tag{7}$$

Here, $\mathbf{r}_{ij} \cdot \mathbf{f}_{ij} = -r_{ij}\, du(r_{ij})/dr_{ij}$ is the intermolecular pair virial. The configurational average can also be expressed in terms of the two-body distribution function $\rho_2(r_{12})$ as[50]

$$\begin{aligned}P &= \rho kT - \frac{1}{6V}\int d\mathbf{r}_1 d\mathbf{r}_2 r_{12} \frac{du(r_{12})}{dr_{12}} \rho_2(r_{12}) \\ &= \rho kT - \frac{1}{6}\int d\mathbf{r}_{12} r_{12} \frac{du(r_{12})}{dr_{12}} \rho_2(r_{12}). \end{aligned} \tag{8}$$

The two-body density $\rho_2(r_{12})$ is of course related to the pair distribution function $g_2(r_{12})$ through $\rho_2(r_{12}) = \rho^2 g_2(r_{12})$.

For inhomogeneous systems, the density and pressure tensor are functions of the position in the fluid. As was first recognized by Kirkwood and Buff[17] there is more than one way of deforming the volume of an inhomogeneous system, leading to different relations between the various components of the pressure tensor and the derivatives of the pair potential. This can be ascribed to the fact that the configurational part of the pressure (or stress) tensor cannot be defined in a unique way as there is no unambiguous way of deciding which molecular pairs contribute to the stress at a given point $\mathbf{r}$. Following the analysis presented by Schofield and Henderson,[49] we define the α-β component of the pressure tensor as

$$P_{\alpha\beta}(\mathbf{r}) = \rho(\mathbf{r}) kT\delta_{\alpha\beta} + \left\langle \sum_i \sum_{j>i}^{*} r_{ij}^{\alpha} f_{ij}^{\beta} \right\rangle, \tag{9}$$

where the asterisk indicates that the double sum is restricted to those molecular pairs that contribute to the virial (or stress) component at a given *fixed* position $\mathbf{r}$. The ambiguity in the definition of the pressure tensor can also be understood as resulting from the difficulty in specifying where a given intermolecular virial is acting in the fluid, and how it is distributed in that region. For this purpose we define $\xi_{\alpha\beta}(\mathbf{r}, \mathbf{r}_i, \mathbf{r}_j)$ as the *fraction* of the intermolecular virial between a given pair of molecules at $\mathbf{r}_i$ and $\mathbf{r}_j$ to be assigned to position $\mathbf{r}$ when evaluating the α-β component of the pressure tensor. Though completely arbitrary, it follows from its definition that this function satisfies the normalization condition

$$\int d\mathbf{r}\; \xi_{\alpha\beta}(\mathbf{r}, \mathbf{r}_i, \mathbf{r}_j) = 1, \tag{10}$$

when integrated over the volume of the sample. Using this function allows one to define the pressure tensor as the configurational average of the unrestricted sum

$$P_{\alpha\beta}(\mathbf{r}) = \rho(\mathbf{r}) kT\delta_{\alpha\beta} + \left\langle \sum_i \sum_{j>i} r_{ij}^{\alpha} f_{ij}^{\beta} \xi_{\alpha\beta}(\mathbf{r}, \mathbf{r}_i, \mathbf{r}_j) \right\rangle. \tag{11}$$

A possible choice, which is appropriate for homogeneous fluids, would be to distribute the intermolecular virial evenly throughout the system. In this case $\xi_{\alpha\beta}$ would not depend on $\mathbf{r}$ and from Eq. (10) it follows that $\xi_{\alpha\beta} = 1/V$. With this choice, Eq. (11) reduces to the definition of the pressure tensor for a homogeneous fluid given in Eq. (6).

For an inhomogeneous system with a planar interface perpendicular to the z axis, the pressure tensor depends only on the distance z from the interface. In this case it is appropriate to define $\xi_{\alpha\beta}$ as

$$\xi_{\alpha\beta}(\mathbf{r}, \mathbf{r}_i, \mathbf{r}_j) = \frac{1}{\mathcal{A}} \xi_{\alpha\beta}(z, z_i, z_j). \tag{12}$$

Here, $\xi_{\alpha\beta}(z, z_i, z_j)$ represents the fraction of the intermolecular virial between a given pair of molecules at positions z_i and z_j to be assigned at a slab of area $\mathcal{A}$ parallel to the interface and centred at position z. The normalization condition Eq. (10) requires that

Downloaded 10 Oct 2005 to 155.198.160.109. Redistribution subject to AIP license or copyright, see http://jcp.aip.org/jcp/copyright.jsp

$$\int_{-\infty}^{\infty} dz\ \xi_{\alpha\beta}(z,z_i,z_j) = 1. \tag{13}$$

The symmetry of the planar interface also implies that the transverse and normal components are $P_{xx}(z)=P_{yy}(z)=P_T(z)$ and $P_{zz}(z)=P_N(z)$, respectively. From the definition of $\xi_{\alpha\beta}(z,z_i,z_j)$ given in Eq. (12), the tensorial components can be written in the form of Eq. (11) as

$$P_N(z) = \rho(z)kT - \frac{1}{\mathcal{A}}\left\langle \sum_i \sum_{j>i} \frac{z_{ij}^2}{r_{ij}} \frac{du(r_{ij})}{dr_{ij}} \xi_N(z,z_i,z_j) \right\rangle, \tag{14}$$

$$P_T(z) = \rho(z)kT - \frac{1}{\mathcal{A}}\left\langle \sum_i \sum_{j>i} \left(\frac{x_{ij}^2 + y_{ij}^2}{2r_{ij}} \right) \frac{du(r_{ij})}{dr_{ij}} \xi_T(z,z_i,z_j) \right\rangle, \tag{15}$$

where the tangential component has been expressed as $P_T(z)=[P_{xx}(z)+P_{yy}(z)]/2$. Here, ξ_N and ξ_T refer to the appropriate definition of the function ξ for the normal and tangential components, respectively. A judicious (but again not unique) choice of ξ implies an even distribution of the pair virial among all slabs z between z_i and z_j for both the normal and tangential components (Irving-Kirkwood[48] recipe). This is equivalent to taking

$$\xi_N = \xi_T = \xi(z,z_i,z_j) = \int_0^1 d\lambda\ \delta(z - z_i - \lambda z_{ij}) = \frac{1}{|z_{ij}|}[H(z-z_i) - H(z-z_j)], \tag{16}$$

where $\lambda=(z-z_i)/z_{ij}$, and $\delta(x)$ and $H(x)$ are the Dirac delta and Heaviside functions. It is straightforward to check that this choice satisfies the normalization condition Eq. (13). This choice yields the Irving-Kirkwood (IK) definition of the pressure tensor, normally expressed in terms of the two-body distribution function:

$$P_N(z) = \rho(z)kT - \frac{1}{\mathcal{A}}\left\langle \sum_i \sum_{j>i} \frac{z_{ij}^2}{r_{ij}} \frac{du(r_{ij})}{dr_{ij}} \times \int_0^1 d\lambda\ \delta(z - z_i - \lambda z_{ij}) \right\rangle \tag{17}$$

$$= \rho(z)kT - \frac{1}{2\mathcal{A}} \int d\mathbf{r}_1 d\mathbf{r}_{12} \frac{z_{12}^2}{r_{12}} \frac{du(r_{12})}{dr_{12}} \times \int_0^1 d\lambda\ \delta(z - z_1 - \lambda z_{12}) \rho_2(\mathbf{r}_1, \mathbf{r}_{12}), \tag{18}$$

$$P_T(z) = \rho(z)kT - \frac{1}{\mathcal{A}}\left\langle \sum_i \sum_{j>i} \left(\frac{x_{ij}^2 + y_{ij}^2}{2r_{ij}} \right) \frac{du(r_{ij})}{dr_{ij}} \times \int_0^1 d\lambda\ \delta(z - z_i - \lambda z_{ij}) \right\rangle \tag{19}$$

$$= \rho(z)kT - \frac{1}{2\mathcal{A}} \int d\mathbf{r}_1 d\mathbf{r}_{12} \left(\frac{x_{12}^2 + y_{12}^2}{2r_{12}} \right) \frac{du(r_{12})}{dr_{12}} \times \int_0^1 d\lambda\ \delta(z - z_1 - \lambda z_{12}) \rho_2(\mathbf{r}_1, \mathbf{r}_{12}). \tag{20}$$

The definition of Harasima[51] for the pressure tensor follows from the choice

$$\xi_N(z,z_i,z_j) = \int_0^1 d\lambda\ \delta(z - z_i - \lambda z_{ij}) = \frac{1}{|z_{ij}|}[H(z-z_i) - H(z-z_j)], \tag{21}$$

$$\xi_T(z,z_i,z_j) = \delta(z - z_j). \tag{22}$$

The Irving-Kirkwood or Harasima choices yield the same normal component, but differ in the expression of the tangential component, Harasima's convention of placing the whole of the contribution of the virial acting on i at position j being the simpler. The computation of the surface tension with the Harasima recipe appears to lead to larger errors than with the Irving-Kirkwood recipe.[52]

It is also useful to define average (macroscopic) values of the pressure tensor components for an inhomogeneous system as

$$\bar{P}_{\alpha\beta} = \frac{1}{V} \int d\mathbf{r} P_{\alpha\beta}(\mathbf{r}). \tag{23}$$

From the definition given in Eq. (11), it follows that

$$\bar{P}_{\alpha\beta} = \rho kT\delta_{\alpha\beta} + \frac{1}{V}\left\langle \sum_i \sum_{j>i} r_{ij}^{\alpha} f_{ij}^{\beta} \int d\mathbf{r}\ \xi_{\alpha\beta}(\mathbf{r}, \mathbf{r}_i, \mathbf{r}_j) \right\rangle = \rho kT\delta_{\alpha\beta} + \frac{1}{V}\left\langle \sum_i \sum_{j>i} r_{ij}^{\alpha} f_{ij}^{\beta} \right\rangle, \tag{24}$$

which, with the normalization condition Eq. (10), turns out to be independent of the particular choice of function ξ; the average tensor is therefore well defined. It is clear from a comparison with Eq. (6) that expression (24) applies to both homogeneous and inhomogeneous systems. By substituting the expressions (14) and (15) for the components of the pressure tensor into Eq. (1), the surface tension can now be obtained explicitly in terms of the derivative of the pair potential as

Downloaded 10 Oct 2005 to 155.198.160.109. Redistribution subject to AIP license or copyright, see http://jcp.aip.org/jcp/copyright.jsp

$$\gamma = \int_{-\infty}^{\infty} dz[P_N(z) - P_T(z)]$$
$$= L_z[\bar{P}_N - \bar{P}_T]$$
$$= \frac{1}{\mathcal{A}}\left\langle \sum_i \sum_{j>i} \left(\frac{x_{ij}^2 + y_{ij}^2}{2r_{ij}} - \frac{z_{ij}^2}{r_{ij}} \right) \frac{du(r_{ij})}{dr_{ij}} \right\rangle$$
$$= \frac{1}{\mathcal{A}}\left\langle \sum_i \sum_{j>i} \frac{1}{2}\left(1 - \frac{3z_{ij}^2}{r_{ij}^2} \right) r_{ij} \frac{du(r_{ij})}{dr_{ij}} \right\rangle, \quad (25)$$

where L_z is the dimension of the container along the z axis. The last form of the expression, which is particularly convenient for calculation from a simulation, can be seen as a straightforward reformulation of the virial expression. The outer average corresponds to the configurational average (time average in the case of an MD simulation or ensemble average in the case of a MC simulation). It is important to realize that in simulations of a slab of fluid there are two interfaces and $\mathcal{A}$ represents the total area of both surfaces. The mechanical route for the calculation of the surface tension embodied in Eq. (25) is the obvious choice with a MD simulation as the evaluation of the intermolecular pair forces is required to determine the particle trajectories during the course of the simulation.

Just as the virial expression (7) for the pressure of a homogeneous system can be deduced from the equivalent thermodynamic derivative of the free energy with respect to the volume,[53,54] expression (25) for the surface tension can be obtained from the thermodynamic relation (3) for the derivative of the free energy with respect to the area;[51,55,56] a particularly clear demonstration of the equivalence of the mechanical and thermodynamic expressions for the surface tension has been given more recently by Salomons and Mareschal.[57] In the context of a statistical mechanical treatment, the thermodynamic route to the surface tension involves the corresponding derivative of the logarithm of the partition function. It is important to point out, however, that when a thermodynamic free-energy difference method (such as that of Bennett[18] described in Sec. II B) is employed to determine the surface tension (e.g., the work of Miyazaki *et al.*[26]), the free energy is estimated directly from the average of the Boltzmann factor without the need to invoke the pair virials.

The accuracy of the surface tension obtained from a mechanical relation such as that given by Eq. (25) in a typical simulation is about 10% (unless large system sizes and very long runs are undertaken). The large errors associated with the mechanical route can be attributed to the very large value of the tangential component of the pressure tensor in the vicinity of the interface: for a typical fluid at its normal boiling point ($P=1$ bar), $P_T(z)$ is a very peaked and rapidly varying function in the interfacial region with an average value of about -200 bar;[1] as the interfacial thickness is small (~ 1 nm) compared with the typical cell dimensions employed in a simulation (~ 30 nm), the accuracy of the numerical integration involved in Eq. (25) tends to be poor. This is increasingly true for complex polyatomic systems (e.g., see Ref. 58).

As stated in Sec. II a major problem with the mechanical route for systems interacting through discontinuous potentials is that the derivative of the potential at the point of discontinuity is also discontinuous and has to be represented by a delta function. An estimate of the delta function must therefore be made to evaluate the surface tension from Eq. (25). This means that the mechanical relation is difficult to use for systems comprising molecules interacting through truncated forms of the LJ potential or the square-well potential. A thorough study of the effect on the vapor-liquid surface tension of truncating the LJ potential has been made by Trokhymchuk and Alejandre[34] for spherically truncated LJ interactions by both molecular-dynamics and Monte Carlo simulation. They demonstrate that in the absence of a term which accounts for the "impulsive" effect of the potential at the point of truncation, the spherically truncated (ST) potential is equivalent to the spherically truncated and shifted (STS) potential. The treatment or otherwise of the discontinuity has a significant effect on the calculated value of the surface tension. This contribution was ignored in much of the earlier literature apart from the work by Chapela *et al.*[29,31] In the case of interactions decaying to zero with distance (such as the LJ model) the difference between the ST and STS versions of the potential decreases with the radius of truncation. However, the contribution due to the discontinuity is not, as was commonly believed, correctly accounted for in the analytical tail corrections used to map the surface-tension data from simulations of systems with a truncated potential to that of the full LJ potential. The problem is particularly acute in the case of the square-well potential which is discontinuous both at contact and at the limit of the attractive interaction. The accuracy of the surface tension obtained for the square-well fluid from an expression such as Eq. (25) is highly dependent on one's ability to estimate the corresponding delta functions during the course of the simulation. Orea *et al.*[45,46] have recently reported accurate data for the vapor-liquid surface tension of square-well systems of range $\lambda/\sigma = 1.5$, 2, and 3 from Monte Carlo simulation estimating the virial contributions with the method of Trokhymchuk and Alejandre.[34] One should note that though the mechanical expression (25) is written in a configurational form in terms of the derivatives of the pair potential (which is proportional to the force $\mathbf{f}_{ij}$), it can also be written in an impulsive form in the case of the square-well potential because the forces only change at the points of the discontinuity (collision). If one denotes the change in momentum of particle i with particle j at the point of collision by $\Delta\mathbf{p}_{ij} \propto \mathbf{f}_{ij}$ then the mechanical expression for the surface tension can be written in kinetic form as

$$\gamma = \frac{1}{\mathcal{A}} \frac{1}{t_{\text{sim}}} \sum_{\text{collisions}} \left[z_{ij}\Delta p_{z,ij} - \frac{1}{2}(x_{ij}\Delta p_{x,ij} + y_{ij}\Delta p_{y,ij}) \right]. \quad (26)$$

The sum is now over all collisions for all pairs of particles occurring in the time t_{sim} of the MD simulation. In the case of spherically symmetric discontinuous potentials such as the square well, impulsive (collision-by-collision) MD simulation offers a significant advantage for accurate estimates of

Downloaded 10 Oct 2005 to 155.198.160.109. Redistribution subject to AIP license or copyright, see http://jcp.aip.org/jcp/copyright.jsp

the surface tension.[47] However, this type of approach is difficult to implement for systems comprising nonspherical particles or larger more complex molecules.

B. Thermodynamic free-energy difference

A glance at the thermodynamic relation given by Eq. (4) immediately suggests that the surface tension can be obtained by computing the contribution to the free energy due to the formation of the interface. It is possible to formulate different procedures to estimate such a free-energy difference by molecular simulation. Here, we distinguish free-energy difference methods from free-energy perturbation methods; the latter will be discussed in Sec. II D. The simulation of free-energy differences has been discussed in some detail in the excellent papers by Kofke and Cummings,[59,60] who refer to these as multistage free-energy approaches. The method developed by Bennett[18] (also known as the acceptance ratio method) was the first to be applied to the computation of the surface tension of continuum systems.[26,57] More recently, Moody and Attard[61] have proposed a free-energy difference approach based on the so-called ghost interface theory which is applicable to curved interfaces. Though not as relevant to our paper, it is also important to acknowledge the simulation studies of the interfacial tension of coexisting spin systems such as Ising and Potts models, where a number of closely related free-energy difference methods (including thermodynamic integration) have been employed (e.g., see Refs. 62–67).

In the formalism of Bennett one starts with the usual expression for the Helmholtz free energy in terms of the canonical partition function Q,[50]

$$A = -kT \ln Q, \tag{27}$$

where

$$Q = \frac{1}{N!\,\Lambda^{3N}} \int d\mathbf{r}^N \exp(-U/kT) = \frac{Z}{N!\,\Lambda^{3N}} \tag{28}$$

is the partition function, $Z = \int d\mathbf{r}^N \exp(-U/kT)$ is the configurational integral, $U(\mathbf{r}^N)$ is the configurational energy which is a function of the configurational space $\mathbf{r}^N$, and Λ is the de Broglie wavelength. The probability of finding any arrangement of the N particles in an element of configurational space $d\mathbf{r}^N$ is $N!\mathcal{P}(\mathbf{r}^N)d\mathbf{r}^N$ where the probability density $\mathcal{P}(\mathbf{r}^N)$ is simply

$$\mathcal{P}(\mathbf{r}^N) = \frac{1}{Q}\frac{\exp(-U/kT)}{N!\,\Lambda^{3N}} = \frac{\exp(-U/kT)}{Z}. \tag{29}$$

It follows that the configurational average of a general function $F(\mathbf{r}^N)$ in the canonical ensemble is given by

$$\langle F \rangle = \frac{\int d\mathbf{r}^N F \exp(-U/kT)}{Z}. \tag{30}$$

The Helmholtz free-energy difference $\Delta A_{0\to 1} = A_1 - A_0$ between two arbitrary systems 0 and 1, characterized by configurational energies $U_0(\mathbf{r}^N)$ and $U_1(\mathbf{r}^N)$, can be expressed as the identity[18,21]

$$\begin{aligned}
\Delta A_{0\to 1} &= -kT \ln\left(\frac{Q_1}{Q_0}\right) \\
&= -kT \ln\left(\frac{Z_1}{Z_0}\right) \\
&= -kT \ln\left(\frac{\int d\mathbf{r}^N W \exp(-U_1/kT)\exp(-U_0/kT)/Z_0}{\int d\mathbf{r}^N W \exp(-U_1/kT)\exp(-U_0/kT)/Z_1}\right) \\
&= -kT \ln \frac{\langle W \exp(-U_1/kT)\rangle_0}{\langle W \exp(-U_0/kT)\rangle_1},
\end{aligned} \tag{31}$$

where $Z_0 = \int d\mathbf{r}^N \exp(-U_0/kT)$ and $Z_1 = \int d\mathbf{r}^N \exp(-U_1/kT)$ are the corresponding configurational integrals, and $W(\mathbf{r}^N)$ is an arbitrary weighting function which also depends on the configurational space. According to Eq. (31), the difference $\Delta A_{0\to 1}$ can be obtained from suitable configurational averages obtained by independently sampling systems 0 and 1. The subscripts on the angular brackets denote the system over which the ensemble average is performed. Note that the free-energy difference depends on $W(\mathbf{r}^N)$. Bennett's scheme corresponds to choosing the function $W_m(\mathbf{r}^N)$ that minimizes the variance in the estimate of the ratio Z_1/Z_0 (and hence the estimate of the free-energy difference). By assuming a near Gaussian distribution of the variance and inserting the resulting $W_m(\mathbf{r}^N)$ into Eq. (31), Bennett shows that the ratio Z_1/Z_0 can be expressed as

$$\frac{Z_1}{Z_0} = \frac{\langle \mathcal{F}(+\Delta U/kT + C)\rangle_0}{\langle \mathcal{F}(-\Delta U/kT - C)\rangle_1} \exp(C), \tag{32}$$

where $\mathcal{F}(x) = 1/[1+\exp(-x)]$ is the Fermi function, and $\Delta U = U_1 - U_0$ is the difference in the configurational energy. The "constant" C is obtained from the relation

$$C = \ln\left(\frac{Z_1}{Z_0}\frac{n_0}{n_1}\right). \tag{33}$$

Here, n_0 and n_1 are the numbers of statistically independent configurations generated in each of the Markov chains. Assuming $n_0 = n_1$ self-consistency between Eqs. (31) and (32) requires that

$$\langle \mathcal{F}(-\Delta U/kT - C)\rangle_1 = \langle \mathcal{F}(+\Delta U/kT + C)\rangle_0. \tag{34}$$

This implicit equation for C is solved iteratively to yield the free-energy difference directly from $\Delta A_{0\to 1} = -kTC$. In practice this involves the construction of histograms for the probability distributions of ΔU in systems 0 and 1 from parallel simulations, and numerically determining the value of C that best satisfies Eq. (34). The method of Bennett for computing the free-energy difference is thus a multistage approach, where at least two systems have to be simulated. The overall benefit of the method is that one preferentially samples the region between the two states to provide the best possible estimate of the free-energy difference; this would not be the case if one employed the usual Metropolis distribution.

The method of Bennett was employed by Miyazaki *et al.*[26] to calculate the dominant cost in free energy of forming a vapor-liquid interface for the Lennard-Jones fluid close to its triple point. Their strategy relies on calculating the reversible work required to create an interface in the bulk liquid.

Downloaded 10 Oct 2005 to 155.198.160.109. Redistribution subject to AIP license or copyright, see http://jcp.aip.org/jcp/copyright.jsp

The process was carried out in two stages. During the first stage, the bulk liquid was slowly separated into two interacting slabs of liquid each contained between "transparent" hard walls perpendicular to the direction of separation. In practice, Miyazaki *et al.* examined 17 intermediate states until the distance between the liquid slabs exceeded the range of the interactions so that the particles in the different slabs did not interact with each other. The free-energy difference of each intermediate step was calculated by implementing Bennett's method. During the second stage, the hard walls confining the particles in one of the liquid slabs were slowly removed in opposite directions. The final configuration corresponds to an unconstrained liquid slab in coexistence with its vapor. The free energy associated with the second "relaxation" process was obtained by numerically integrating the derivative of the free energy with respect to the position of the hard wall. The total cost in the free energy of forming the vapor-liquid interface (surface free energy) is thus the sum of the contributions for the two stages. Miyazaki *et al.* estimated the surface tension from the surface Helmholtz free energy using Eq. (4) (where in the case of coexisting vapor v and liquid l phases $A^s = A - A^v - A^l$), rather than from the derivative given in thermodynamic relation (3). The same route to the interfacial tension was employed by Moody and Attard,[61] and in the studies with lattice models.[62–67] Strictly, the surface Helmholtz free energy $A^s = \mu N^s + \gamma \mathcal{A}$ can only be equated with $\gamma \mathcal{A}$ for an appropriate position of the interface (Gibbs dividing surface) such that the surface number of particles $N^s = 0$.[1] The value of the vapor-liquid surface tension obtained by Miyazaki *et al.*[26] for the Lennard-Jones system close to its triple point is about 15% higher than the more recent estimates of the value (e.g., see the corresponding data of Salomons and Mareschal[57]), while an error bar of less than 2% was quoted. Miyazaki *et al.*[26] suggested that the discrepancy (overestimate) found with the experimental value for argon was most likely due to the lack of a proper description of the intermolecular potential with the neglect of three-body interactions. The overestimate seen for the pairwise LJ potential clearly has nothing to do with three-body interactions, and is probably due to their assumption that the term μN^s can be neglected in the evaluation of the surface tension from the surface free energy.

The thermodynamic derivative Eq. (3) is easier to use in calculations of the surface tension as one does not have to make an assumption about the position of the interface. A much simpler two-system simulation has been employed by Salomons and Mareschal[57] to determine the surface tension of the LJ fluid: the difference in the free energy of two systems with slightly different interfacial areas (but with the same overall volume) was determined using the recipe of Bennett, and γ was estimated directly by finite difference to an accuracy of 5%–10% using relation (3). The use of this type of finite difference method will be discussed in more detail in Sec. II D. We should note that though the two-state approach taken by Salomons and Mareschal is simpler than the multistage approach proposed by Miyazaki *et al.*, it still involves an *a posteriori* analysis of the probability distributions obtained from the two simulations to determine the free-energy difference and hence the surface tension. Such a method is thus more laborious than a mechanical approach. The mechanical route can be argued to be more direct as the method involves the evaluation of an average within a single simulation. Simulations of the surface tension with methods based on the approach of Bennett do not, however, suffer from the problems associated with discontinuous potentials. The same is true of our free-energy perturbation method. Before we go on to the advantages of our test-area approach, we describe methods for simulating the surface tension from an analysis of the system-size dependence.

C. Finite-size scaling

A different perspective to estimating the surface tension from a free-energy difference was developed by Binder[19] in the context of a Landau free energy.[68,69] The Landau approach provides a unified framework for the study of phase transitions, where instead of describing the system in microscopic detail one characterizes its state in terms of a macroscopic order parameter. Binder determines the surface tension (or more precisely the surface free energy) of an Ising lattice model of finite size by examining the barrier between the Landau free energy of the coexisting states during the course of a Metropolis Monte Carlo simulation; in this case the magnetization is the appropriate order parameter. The surface tension of the infinite system can then be estimated by extrapolation using a simple scaling relation obtained from a Gaussian distribution. This type of approach has been used to estimate the free-energy barriers of both Ising and Potts lattice models by multicanonical Monte Carlo simulation which provides much more accurate estimates of the surface free energy,[70–74] and has also been used to examine lattice models of freestanding polymer films.[75]

As far as continuum systems are concerned the Landau approach has been used to determine the free-energy difference between liquid and solid phases from isothermal-isobaric simulations of soft spheres[76] and ductile metals;[77] the focus of these studies was to examine the stable solid states of the system, and though the surface free energy was calculated no attempt was made to estimate the value of the surface tension for the infinite system. A similar method was used more recently by Allen *et al.*[78,79] in very interesting studies of the absorption of water and ions in nanoporous channels; in this case grand canonical Monte Carlo simulation is the appropriate technique to determine the free-energy barrier for the confined system. The vapor-liquid surface tension of a Lennard-Jones fluid has been estimated from the Landau free-energy barrier using the scaling approach of Binder by both isothermal-isobaric[80] and grand canonical[81,82] Monte Carlo simulation; in these studies biased sampling techniques including multicanonical, umbrella, and transition matrix methods were used to improve the accuracy particularly at low temperatures. Systems of particles interacting through discontinuous square-well potentials have also been simulated in a similar way to determine the vapor-liquid coexistence and surface tension.[47]

Before the approach of Binder for the estimation of the surface tension from the Landau free-energy profile is outlined it is useful to make the link between Landau's phenom-

Downloaded 10 Oct 2005 to 155.198.160.109. Redistribution subject to AIP license or copyright, see http://jcp.aip.org/jcp/copyright.jsp

enological theory and the statistical mechanical formalism employed in the previous sections. We choose the grand canonical ensemble to illustrate the method as the use of a Landau free energy has already been described within this ensemble (e.g., see Ref. 79), and because the grand potential $\Omega = A - N\mu$ is particulary convenient for studies of interfacial systems. The grand canonical ensemble corresponds to a system at constant temperature T, volume V, and chemical potential μ. The grand canonical partition function is written in the usual microscopic form as[50]

$$\Xi = \sum_{N=0}^{\infty} \frac{1}{N!\,\Lambda^{3N}} \exp(\mu N/kT) \int d\mathbf{r}^N \exp(-U/kT) = \sum_{N=0}^{\infty} \exp(\mu N/kT) Q(N), \tag{35}$$

where $Q(N)$ is the canonical partition function for the system of N particles given by Eq. (28). The connection with thermodynamics is made through the relevant thermodynamic potential Ω,

$$\Omega = -kT \ln \Xi = -PV. \tag{36}$$

In the grand canonical ensemble the probability density $\mathcal{P}(\mathbf{r}^N; N)$,

$$\mathcal{P}(\mathbf{r}^N; N) = \frac{1}{N!\,\Lambda^{3N}\Xi} \exp(\mu N/kT) \exp(-U/kT), \tag{37}$$

is proportional to the probability of finding exactly N particles in an element of configurational space $d\mathbf{r}^N$.

A convenient order parameter for this ensemble is the number of particles (now denoted as N^* to distinguish it from the index of the sum over particles) as it varies during the course of a grand canonical simulation in a way that maintains the chemical potential constant. A restricted grand canonical partition function $\Xi(N^*)$ for systems containing just N^* particles can be defined as

$$\begin{aligned}\Xi(N^*) &= \sum_{N=0}^{\infty} \frac{1}{N!\,\Lambda^{3N}} \exp(\mu N/kT) \times \int d\mathbf{r}^N \exp(-U/kT)\,\delta(N - N^*) \\ &= \sum_{N=0}^{\infty} \exp(\mu N/kT) Q(N)\,\delta(N - N^*) \\ &= \exp(\mu N^*/kT) Q(N^*),\end{aligned} \tag{38}$$

which can clearly be seen to be directly proportional to the canonical partition function $Q(N^*)$ for the system of N^* particles. A Landau "free energy" can now be identified with the corresponding restricted grand potential:

$$\Omega(N^*) = -kT \ln \Xi(N^*). \tag{39}$$

One should note that for this ensemble $\Omega(N^*)$ is more closely related to the pressure than to a free energy. This Landau grand potential thus represents the weighted volume of phase space for states consisting of exactly N^* particles. The probability $\mathcal{P}(N^*)$ of finding exactly N^* particles in any element of configurational space $d\mathbf{r}^{N^*}$ is now

$$\begin{aligned}\mathcal{P}(N^*) &= \frac{1}{N^*!\,\Lambda^{3N^*}\Xi} \exp(\mu N^*/kT) \int d\mathbf{r}^{N^*} \exp(-U/kT) \\ &= \frac{\exp(\mu N^*/kT) Q(N^*)}{\Xi} = \frac{\Xi(N^*)}{\Xi}.\end{aligned} \tag{40}$$

It follows that the restricted grand potential $\Omega(N^*)$ can be expressed in the form of a Landau free energy in terms of the probability $\mathcal{P}(N^*)$ as

$$\Omega(N^*) = -kT \ln \mathcal{P}(N^*) - kT \ln \Xi, \tag{41}$$

where for a given thermodynamic state (μVT), the last term in the logarithm of the grand partition function is just a constant.

The Landau grand potential contains more information than the full grand potential as information about the order parameter is lost in the latter due to the averaging over all phase space. For appropriate choices of the thermodynamic variables μ, V, and T corresponding to the coexistence of two phases α and β (characterized by different values of the order parameter N^*, i.e., two different number densities), the Landau grand potential of a finite-size system develops a double-well shape in the order parameter: the two minima are of equal depth, $\Omega_{\min}(N^*_\alpha) = \Omega_{\min}(N^*_\beta)$, as mechanical equilibrium requires the pressures (and thus the Landau grand potentials) of the coexisting phases to be the same; the probability of being in either of the two coexisting states is thus a maximal point and the same, i.e., $\mathcal{P}_{\max}(N^*) = \mathcal{P}_{\max}(N^*_\alpha) = \mathcal{P}_{\max}(N^*_\beta)$. The two minima in the Landau grand potential are separated by a maximum $\Omega_{\max}(N^*_{\alpha\beta})$ at an intermediate value of the order parameter corresponding to the interfacial configurations; the probability $\mathcal{P}_{\min}(N^*_{\alpha\beta})$ for this intermediate state is thus at a minimum. For a clear discussion of the general behavior of the Landau free energy the reader is directed to the excellent paper of Lee and Kosterlitz.[83] The free-energy barrier represents the difference between the maximum (interface) and the minimum (bulk) values of the Landau free energy, and can thus be used to estimate the surface free energy and interfacial tension, as was first shown by Binder.[19]

The difference in a general Landau free energy $\Delta F_L = F_{\max}(N^*_{\alpha\beta}) - F_{\min}(N^*)$ between states corresponding to the intermediate (heterophase) region and the stable homophases is given by

$$\Delta F_L = -kT \ln \frac{\mathcal{P}_{\min}(N^*_{\alpha\beta})}{\mathcal{P}_{\max}(N^*)}, \tag{42}$$

where the box dimension L dependence is emphasized in the subscript to indicate that this is for a finite system. According to the finite-size scaling analysis of Binder[19] one can assume that in the asymptotic regime of large L,

$$\lim_{L\to\infty} \frac{\mathcal{P}_{\min}(N^*_{\alpha\beta})}{\mathcal{P}_{\max}(N^*)} \propto L^x \exp(-F^s/kT), \tag{43}$$

where the exponent x (which includes capillary waves and other effects) has to be determined, and F^s is the surface free

Downloaded 10 Oct 2005 to 155.198.160.109. Redistribution subject to AIP license or copyright, see http://jcp.aip.org/jcp/copyright.jsp

energy of the infinite system. This means that in this limit the free-energy barrier of the finite-size system [Eq. (42)] can be written as

$$\Delta F_L = F^s - kT\,x \ln L - kT \ln C, \tag{44}$$

which leads to the corresponding expression for the interfacial tension $\gamma = F/\mathcal{A}$:

$$\gamma_L = \gamma - \frac{kT\,x \ln L}{2L^2} - \frac{kTC}{2L^2}. \tag{45}$$

Here, γ_L is the surface tension of the finite-size system determined from the ratio of the probabilities [cf. Eq. (42)], C is a constant of proportionality, and the area $\mathcal{A}=2L^2$ is taken to be that of a planar film (two interfaces) in a cubic three-dimensional box. The surface tension γ of the infinite system, which is the property of interest, can thus be obtained by a linear extrapolation of the data from a series of finite-size simulations for different values of L: a plot of γ_L vs $\ln(L)/(2L^2)$ will yield γ in the limit $L \to \infty$. In the case of a canonical ensemble, the appropriate thermodynamic potential is the Helmholtz free energy ($F \equiv A$) and one is essentially obtaining the surface tension from the surface Helmholtz free energy defined in Eq. (4), $A^s = \mu N^s + \gamma\mathcal{A} \approx \gamma\mathcal{A}$, by assuming that the term in N^s is negligible. Though this does not appear to be a major problem in simulations of lattice models, such an assumption may not be appropriate in the case of simulations of continuum systems, as has already been discussed in Sec. II B. Lynden-Bell *et al.*[77] have pointed out that the same type of approximation is made in simulations in the isothermal-isobaric ensemble (now $F \equiv G$), where one can estimate the surface tension from the surface Gibbs free energy, $G^s \approx \gamma\mathcal{A}$. The grand canonical ensemble offers a distinct advantage in simulations of the surface tension because in this case the Landau free energy represents a grand potential ($F \equiv \Omega$), and the surface grand potential is always given by $\Omega^s = \gamma\mathcal{A}$ [cf. Eq. (5)] regardless of the choice of dividing surface.[1] This may account for the small differences in the values found for the vapor-liquid surface tension of the Lennard-Jones system with the Binder method from simulations in the isothermal-isobaric[80] and grand canonical[81,82] ensembles, though it is likely that system-size effects are also a cause of the discrepancy.

It is important to point out a key complication with this type of approach. Near the critical point the simulated configurations fluctuate easily between the two coexisting states, and the intermediate interfacial region is easily sampled. However, as the temperature is lowered from the critical point, the configurations sampled are predominantly those of either of the coexisting phases and it becomes increasingly difficult to sample the intermediate states to estimate $\mathcal{P}(N^*)$ (and hence the surface tension) with any accuracy. A non-Boltzmann Monte Carlo scheme such as the umbrella sampling method of Torrie and Valleau[84] or the multicanonical method of Berg *et al.*[70] can be used to increase the frequency of sampling the low-probability states with large Landau free energy. In the case of the umbrella sampling technique, the configurations in the Markov chain are sampled with a biased probability

$$\mathcal{P}_{\text{bias}}(N^*) = \frac{\mathcal{P}(N^*)W(N^*)}{\langle W(N^*)\rangle}, \tag{46}$$

where $W(N^*)$ is a biasing weight function which is chosen to provide a sampling which is as even as possible over an appropriate range of the order parameter (e.g., see Refs. 21, 76, and 79 for more details). The weight function plays an analogous role to the one introduced by Bennett[18] for the determination of the difference in the free energy of a system in two different states (see Sec. II B). The Landau grand potential $\Omega(N^*)$ of the unbiased system is obtained from the biased simulation by reexpressing Eq. (41) in terms of the biased probability $\mathcal{P}_{\text{bias}}(N^*)$ defined in Eq. (46),

$$\begin{aligned}\Omega(N^*) &= -kT \ln \mathcal{P}_{\text{bias}}(N^*) + kT \ln W(N^*) - kT \ln\langle W(N^*)\rangle \\ &\quad - kT \ln \Xi = -kT \ln \mathcal{P}_{\text{bias}}(N^*) + kT \ln W(N^*) + K,\end{aligned} \tag{47}$$

where the last two terms can be combined into a constant K that depends on the thermodynamic variables. The use of such a biasing technique provides a good representation of the Landau free energy in the low-probability intermediate region, and accurate estimates of the interfacial tension are possible, at least for temperatures not too far below the critical point.[80–82]

The benefit of this type of method is that, in common with other thermodynamic approaches, no derivatives of the potential are required to determine the surface tension. As the bulk and interfacial states are sampled during the course of the simulation there is also no need to establish an interfacial profile. In view of the fact that the method is based on finite-size scaling techniques, it can also be used to provide information about the critical region such as the critical exponents. There are, however, several disadvantages with the Binder approach. The first is that the coexistence conditions must be known (or determined) beforehand; this is not a problem for well-characterized systems such as the Lennard-Jones or square-well fluid but can be a major issue in simulations of complex fluids and mixtures. Another disadvantage is that a number of simulations must be performed for each thermodynamic state, as the data has to be scaled to obtain an estimate for the system of infinite area; with the advent of routine parallel computing this issue has become less problematic. More significantly, the probability of sampling the interfacial configurations is so low in the case of low-temperature states (less than ~75% of the critical point) that the surface tension cannot be computed to any degree of accuracy in the region of the triple point even with biased sampling techniques (see Refs. 80 and 81). The form of weighting function is not usually known *a priori* and must be chosen carefully to give accurate low-temperature data. Errington[82] has recently used a transition matrix Monte Carlo method (which allows one to assess the configurations with very low probability) to extend the applicability of the Binder finite-size scaling approach for the surface tension of the Lennard-Jones system to temperatures as low as the triple point, but such an approach does not appear to provide a distinct advantage for the square-well system.[47] As Potoff and Panagiotopoulos[81] remark, the Binder approach should

Downloaded 10 Oct 2005 to 155.198.160.109. Redistribution subject to AIP license or copyright, see http://jcp.aip.org/jcp/copyright.jsp

be viewed as a complementary method which is particularly suited to studies of the near-critical region.

A discussion of the techniques used to simulate the surface tension would not be complete without a mention, albeit brief, of phenomenological approaches based on the capillary-wave theory.[1,20,85–87] In a capillary-wave picture one examines density fluctuations of the interface in terms of a Fourier series of the displacement from a mean position. The free energy of the deformation due to the associated capillary waves can be viewed as a type of Landau free energy (or interface Hamiltonian) with the vertical displacement playing the role of the order parameter. For long-wavelength distortions, the interface Hamiltonian can be linearized and one finds that the mean-square fluctuation from the mean position (the square of the interfacial thickness) depends on the logarithm of the area of the system, $\langle z^2\rangle \propto (kT/\gamma)\ln \mathcal{A}$. By computing the mean-square displacement of the interface from a series of simulations for systems of different sizes $\mathcal{A}=L^2$ (or from a discretization of a large simulation cell into a number of subsystems) one can estimate the surface tension of the infinite system. The capillary-wave model provides a particularly useful way of describing the long-wavelength fluctuations of the interface. There are, however, a number of controversies surrounding the approach. As has been pointed out by Gelfand and Fisher[87] in their very thorough review, capillary-wave theories do not provide a complete description of equilibrium interfaces: there are difficulties associated with the short-wavelength distortions of the system, and the approach is inadequate in describing the Tolman correction to the tension of curved interfaces. The former could be part of the reason for inconsistencies in some of the reported simulation data: for example, the surface tension of the isotropic-nematic interface estimated by Akino *et al.*[13] using the capillary-wave formalism is about half that computed from the mechanical relation [cf. Eq. (1)].

D. Thermodynamic free-energy perturbation: New test-area approach

Our new method for the direct simulation of the surface tension is related to the thermodynamic approach discussed in Sec. II B, where one employs the recipe of Bennett[18] to evaluate the free-energy difference from simulations of two systems with different interfacial areas. By contrast we evaluate the change in the free energy from test perturbations in the area of the system within a single simulation. The test state is used to evaluate the free-energy perturbation but does not otherwise affect the properties of the reference system of interest. A close analogy can be made with the Widom[88] potential distribution method for the calculation of the chemical potential by examining test-particle insertions (or deletions). Kofke and Cummings[59,60] have classified such perturbative approaches as single-stage methods, to which our method conforms.

The development of a statistical mechanical framework for this type of free-energy perturbation owes much to the early papers of Longuet-Higgins,[89] Barker,[90,91] Pople,[92,93] and Zwanzig.[94] Longuet-Higgins[89] developed a perturbation approach for mixtures of conformal fluids that went beyond regular solution theory, while the focus of the work by Barker[90,91] and Pople[92,93] was on perturbation theories of dipolar fluids based on a nonpolar reference. A more general formalism of the perturbative approach was first outlined by Zwanzig,[94] and it is this seminal paper that we use as the starting point for the description of our test-area method.

As we have already seen in Sec. II B, the difference in the Helmholtz free energy of two systems labeled 0 and 1 can be expressed in terms of the ratios of their canonical partition functions Q_0 and Q_1 simply as

$$\Delta A_{0\to 1} = A_1 - A_0 = -kT\ln\left(\frac{Q_1}{Q_0}\right). \tag{48}$$

In the case of two systems with the same number of particles of the same species at the same volume and temperature, the ratio Q_1/Q_0 is equivalent to the ratio Z_1/Z_0 of the configurational integrals $Z_0=\int d\mathbf{r}^N \exp(-U_0/kT)$ and $Z_1=\int d\mathbf{r}^N \times\exp(-U_1/kT)$:

$$\frac{Q_1}{Q_0}=\frac{Z_1}{Z_0}=\frac{\int d\mathbf{r}^N \exp(-U_1/kT)}{\int d\mathbf{r}^N \exp(-U_0/kT)}. \tag{49}$$

The configurational energy $U_1(\mathbf{r}^N)$ of system 1 can be assumed to be a "perturbation" to the configuration energy $U_0(\mathbf{r}^N)$ of the "reference" system 0, $U_1=U_0+\Delta U$, where ΔU is the difference in the potential energy. By applying the expression (30) for the average of a general function of configurational space in the canonical ensemble, the ratio Z_1/Z_0 can now be expressed in terms of an average solely over the reference system 0 as

$$\frac{Z_1}{Z_0}=\frac{\int d\mathbf{r}^N \exp(-U_0/kT)\exp(-\Delta U/kT)}{\int d\mathbf{r}^N \exp(-U_0/kT)} = \langle \exp(-\Delta U/kT)\rangle_0. \tag{50}$$

One should emphasize that $\Delta U=U_1-U_0$ corresponds to a test perturbation from the reference system and does not otherwise affect its properties during the computation of the average. The free-energy difference $\Delta A_{0\to 1}$ is thus simply proportional to the logarithm of the Boltzmann factor of ΔU averaged over the configurations of the reference state:

$$\Delta A_{0\to 1} = -kT\ln\langle \exp(-\Delta U/kT)\rangle_0. \tag{51}$$

This is the well-known general result derived by Zwanzig.[94] It is interesting to note that when the weighting function in the relation obtained by Bennett, Eq. (31), is chosen such that $W=\exp(+U_0/kT)$, one recovers the Zwanzig result, Eq. (51). The Zwanzig expression is valid for any difference in the configurational energy, though in practice only moderate perturbations provide good statistics for the ratio Z_1/Z_0 and hence the free-energy difference; the approach of Bennett can be employed to remedy this (see Sec. II B). There is also no guarantee that the free energy of the perturbed system corresponds to the equilibrium state with the minimum free energy when the difference in potential energy is large. For small values of the perturbation (relative to kT) both the exponential and logarithm of Eq. (51) can be expanded, and the free-energy perturbation can be expressed in the form of Zwanzig's high-temperature expansion as[94]

Downloaded 10 Oct 2005 to 155.198.160.109. Redistribution subject to AIP license or copyright, see http://jcp.aip.org/jcp/copyright.jsp

$$\Delta A_{0\to 1} = \langle \Delta U \rangle_0 - \frac{\langle \Delta U^2 \rangle_0 - \langle \Delta U \rangle_0^2}{2\,!\,(kT)} + \frac{\langle \Delta U^3 \rangle_0 - 3\langle \Delta U^2 \rangle_0 \langle \Delta U \rangle_0 + 2\langle \Delta U \rangle_0^3}{3\,!\,(kT)^2} - \cdots, \tag{52}$$

where the first term is the mean-attractive perturbative energy, the second is the fluctuation term, and the third characterizes the asymmetry in the distribution of the potential-energy difference. In the early papers of Longuet-Higgins,[89] Barker,[90,91] and Pople,[92,93] the free-energy perturbation tended to be expressed in a linear form corresponding only to the first term, or included only the first few terms in the series. This type of expansion is the basis for a number of modern perturbation theories of fluids (e.g., see Ref. 50), but is strictly only valid for small perturbations in the configurational energy where the series converges. The exact unexpanded relation (51) is the key to our test-area approach for the determination of surface tension from numerical simulation.

Before we develop our approach it is useful to discuss the Widom[88] test-particle method for the determination of the chemical potential in the context of the Zwanzig relation. Though the test-particle method is usually attributed solely to Widom, it was developed independently by Jackson and Klein[95] at about the same time, and had been formulated earlier by Byckling[96] for the special case of hard spheres. The thermodynamic definition of the chemical potential μ of a pure homogeneous system can be obtained from the free-energy change Eq. (2) as

$$\mu = \left(\frac{\partial A}{\partial N}\right)_{V,T} = \lim_{\Delta N \to 0} \left(\frac{\Delta A}{\Delta N}\right)_{V,T}. \tag{53}$$

In the thermodynamic limit ($N \to \infty$) we can thus equate the chemical potential for a system of N particles at constant volume V and temperature T with the difference in the Helmholtz free energy of systems with $N+1$ and N particles: $\mu = \lim_{N\to\infty} \Delta A = \lim_{N\to\infty} (A_{N+1} - A_N)$. In this case the system with N particles can be regarded as the reference system 0, and that with $N+1$ particles the perturbed system 1. From the formal statistical mechanical relation between the partition functions of the two systems, the difference in the Helmholtz free energy given by Eq. (31) can be expressed as

$$\Delta A_{0\to 1} = A_{N+1} - A_N = -kT \ln \frac{Q_1}{Q_0} = -kT \ln \frac{Z_1/[(N+1)\,!\,\Lambda^{3(N+1)}]}{Z_0/[N\,!\,\Lambda^{3N}]}. \tag{54}$$

The canonical partition functions Q_0 and Q_1 are written in terms of the configurational integrals $Z_0 = \int d\mathbf{r}^N \exp(-U_0/kT)$ and $Z_1 = \int d\mathbf{r}^{N+1} \exp(-U_1/kT)$ using the corresponding relations (28), where in this case the configurational energies are $U_0 = U_N(\mathbf{r}^N)$ and $U_1 = U_{N+1}(\mathbf{r}^{N+1})$. In an analogous way to the approach followed by Zwanzig, the ratio of the configurational integrals can be written in terms of the average Boltzmann factor of the difference $\Delta U = U_1 - U_0$ in the configurational energy (test potential energy):

$$\frac{Z_1}{Z_0} = \frac{\int d\mathbf{r}^{N+1} \exp(-U_1/kT)}{\int d\mathbf{r}^N \exp(-U_0/kT)} = \frac{\int d\mathbf{r}_1 \int d\mathbf{r}^N \exp(-U_0/kT)\exp(-\Delta U/kT)}{\int d\mathbf{r}^N \exp(-U_0/kT)} = V\langle \exp(-\Delta U/kT)\rangle_0. \tag{55}$$

Apart from the volume prefactor, which appears because the position of the test particle (particle 1) is taken as the origin and integrated over all spaces, this expression is identical to that of Zwanzig [cf. Eq. (50)]. The average denotes a canonical average over all configurations of the N particles in the reference state (system 0) and over all positions of the test particle. For a large enough system the chemical potential is then obtained from the free-energy difference Eq. (54) as

$$\mu = \lim_{N\to\infty} \Delta A_{0\to 1} = kT \ln[(N+1)\Lambda^3/V] - kT \ln\langle \exp(-\Delta U/kT)\rangle_0, \tag{56}$$

in which one can recognize the ideal (first term) and residual (second term) contributions. The implementation of the Widom test-particle method for the determination of the chemical potential thus involves the evaluation of the average Boltzmann factor of the test-particle potential energy during the course of a single simulation. Here, we have described a test-particle insertion approach rather than the equivalent deletion approach which can be developed in an analogous manner from the corresponding free-energy difference $\Delta A_{1\to 0}$; system 1 with $N+1$ particles is now taken as the reference and system 0 with N particles is the perturbed state. There are inherent problems with the implementation of the deletion (and to a lesser extent the insertion) method particularly for systems of hard-core particles due to the asymmetry in the insertion/deletion free-energy difference $\Delta A_{0\to 1} \neq -\Delta A_{1\to 0}$ (the reader is referred to the papers of Kofke and Cummings[59,60] for a recent discussion). This type of problem will be discussed in the context of our test-area approach for the vapor-liquid interfacial tension of the square-well fluid.

We now return to the computation of the surface tension which can be obtained from the change in free energy in the limit of an infinitesimal perturbation in the area [cf. Eq. (3)],

$$\gamma = \left(\frac{\partial A}{\partial \mathcal{A}}\right)_{N,V,T} = \lim_{\Delta \mathcal{A} \to 0} \left(\frac{\Delta A}{\Delta \mathcal{A}}\right)_{N,V,T}. \tag{57}$$

Though our method is general and can be applied to different types of interfaces in pure systems and mixtures, for illustrative purposes we describe the approach in the special case of a vapor-liquid interface of a pure fluid. A standard Metropolis Monte Carlo (or molecular-dynamics) simulation of a system of N particles is performed at a temperature T in a volume $V = L_x L_y L_z$, where L_x, L_y, and L_z are the dimensions of the rectangular simulation cell.[21] A homogeneous liquid state is first equilibrated in a cubic box, and then two empty cubic boxes (vacuum) are placed either side of the final liquid configuration. If the temperature and overall number density $\rho = N/V$ are chosen to be well within the vapor-liquid coexistence envelope, the system retains its inhomogeneity in the density and relaxes to form a planar liquid film of area $\mathcal{A}$

Downloaded 10 Oct 2005 to 155.198.160.109. Redistribution subject to AIP license or copyright, see http://jcp.aip.org/jcp/copyright.jsp

coexisting with its vapor. By choosing an appropriate number of particles and setting the box dimensions such that $L_z = 3\,L_x = 3\,L_y$ one can ensure that the two vapor-liquid interfaces stay parallel to the x-y plane with an overall interfacial area of $\mathcal{A} = 2\,L_x L_y$. There is no need to establish the coexistence conditions precisely at the start, as the densities of the coexistence vapor and liquid phases can be obtained by analyzing the density profile $\rho(z)$ perpendicular to the interface. The system must first be simulated to properly equilibrate this reference state (system 0) with interfacial area $\mathcal{A}_0 = 2\,L_{x,0}L_{y,0}$. A test-area change is then performed to generate a perturbed state (system 1) with a new surface area $\mathcal{A}_1 = \mathcal{A}_0(1+\Delta\mathcal{A}^*)$ such that the overall volume of the system is maintained; the dimensionless parameter $\Delta\mathcal{A}^*$ which is set at the start of the simulation and characterizes the small fractional change in area $\Delta\mathcal{A} = \mathcal{A}_0\Delta\mathcal{A}^*$, which at this point is assumed to be positive. The perturbation in area is made such that the x and y dimensions change by equal amounts, $L_{x,1} = L_{x,0}\sqrt{(1+\Delta\mathcal{A}^*)}$ and $L_{y,1} = L_{y,0}\sqrt{(1+\Delta\mathcal{A}^*)}$, and the z dimension responds to keep the volume constant, $L_{z,1} = L_{z,0}(1+\Delta\mathcal{A}^*)^{-1}$. The reduced particle coordinates $\mathbf{r}^* = (x/L_x, y/L_y, z/L_z)$ are maintained during this affine transformation in the box shape, i.e., the relative positions in terms of the box axes are retained, $\mathbf{r}_0^* = \mathbf{r}_1^*$. As before the change in the free energy $\Delta A = \Delta A_{0\to1} = A_1 - A_0$ due to the perturbation in area can be expressed in terms of the appropriate ratio of the partition functions (configurational integrals) as

$$\Delta A_{0\to1} = A_1 - A_0 = -kT\ln\left(\frac{Q_1}{Q_0}\right) = -kT\ln\left(\frac{Z_1}{Z_0}\right). \tag{58}$$

The configurational integrals $Z_0 = \int d\mathbf{r}^N \exp(-U_0/kT)$ and $Z_1 = \int d\mathbf{r}^N \exp(-U_1/kT)$ now represent those of a reference system 0 with an area $\mathcal{A}_0$ and configurational energy $U_0(\mathbf{r}^N)$, and a perturbed system 1 with an area $\mathcal{A}_1$ and configurational energy $U_1(\mathbf{r}^N)$. The ratio of the configurational integrals can again be related directly to the average Boltzmann factor of the perturbation in the configurational energy $\Delta U = U_1 - U_0$:

$$\begin{aligned}\frac{Z_1}{Z_0} &= \frac{\int d\mathbf{r}^N \exp(-U_1/kT)}{\int d\mathbf{r}^N \exp(-U_0/kT)} \\ &= \frac{\int d\mathbf{r}^N \exp(-U_0/kT)\exp(-\Delta U/kT)}{\int d\mathbf{r}^N \exp(-U_0/kT)} \\ &= \frac{V^N \int d\mathbf{r}^{*N} \exp(-U_0/kT)\exp(-\Delta U/kT)}{V^N \int d\mathbf{r}^{*N} \exp(-U_0/kT)} \\ &= \langle \exp(-\Delta U/kT)\rangle_0. \end{aligned} \tag{59}$$

In evaluating the canonical average over the reference system 0, care must be taken that the integrals over configurational space in the perturbed (numerator) and reference (denominator) states are undertaken in an equivalent fashion when the box shape is changed; this is guaranteed simply by performing the simulation in terms of the usual reduced coordinates $\mathbf{r}^*$ so that sampling over all configurations of the reference ensures an equivalent sampling of configurations in the perturbed system. The use of reduced coordinates also makes the calculation of the configurational energy of the perturbed system (and the corresponding energy change) very efficient. The change in Helmholtz free energy due to a perturbation in area [Eq. (58)] can thus be computed from the Boltzmann factor of the change in configurational energy averaged over the reference system 0 [cf. Eq. (51)]. The surface tension is then simply obtained from Eq. (57) as

$$\gamma = \lim_{\Delta\mathcal{A}\to0}\left(\frac{\Delta A_{0\to1}}{\Delta\mathcal{A}}\right)_{N,V,T} = -\frac{kT}{\Delta\mathcal{A}}\ln\langle\exp(-\Delta U/kT)\rangle_0. \tag{60}$$

One should stress that here the surface tension is obtained as an average from a single simulation, a clear advantage over the free-energy difference techniques discussed in Sec. II B. In common with other perturbation techniques, the test change in area is only used to compute the free-energy difference and does not affect the sampling of the reference system. This means that the underlying simulation can be performed using either a Monte Carlo or molecular-dynamics algorithm. The perturbation in the area should be made small enough so that Eq. (60) is an accurate representation of the interfacial tension, but large enough to provide reasonable statistics for the Boltzmann factor.

Before concluding the description of our method it is useful to take a more detailed look at the numerical evaluation of derivatives such as Eq. (57). Though in practice one cannot make infinitesimal perturbations in the area, a finite difference technique can be used to estimate the derivative.[97] For a continuous function $f(x)$ of the variable x the forward difference (FD) and central difference (CD) expressions for the first derivative of $f(x)$ with respect to x are given by

$$\left(\frac{df}{dx}\right)_{\mathrm{FD}} \approx \left(\frac{\Delta f}{\Delta x}\right)_{\mathrm{FD}} = \frac{f(x+\Delta x) - f(x)}{\Delta x}, \tag{61}$$

$$\left(\frac{df}{dx}\right)_{\mathrm{CD}} \approx \left(\frac{\Delta f}{\Delta x}\right)_{\mathrm{CD}} = \frac{f(x+\Delta x) - f(x-\Delta x)}{2\Delta x}, \tag{62}$$

written here for a given small change Δx. The FD expression corresponds to a zeroth-order approximation, while the CD method represents a first-order expression which is more accurate in general. In our notation the corresponding FD expression for the surface tension can be expressed in terms of the Helmholtz free-energy difference $\Delta A_{0\to1} = A_1(\mathcal{A}_1) - A_0(\mathcal{A}_0)$ of the reference system 0 with area $\mathcal{A}_0$ and the perturbed system with the larger area $\mathcal{A}_1 = \mathcal{A}_0 + \Delta\mathcal{A}$ as

$$\gamma = \left(\frac{\partial A}{\partial\mathcal{A}}\right)_{\mathrm{FD}} \approx \frac{A_1(\mathcal{A}_0+\Delta\mathcal{A}) - A_0(\mathcal{A}_0)}{\Delta\mathcal{A}} = \frac{\Delta A_{0\to1}}{\Delta\mathcal{A}}, \tag{63}$$

which is the same as Eq. (60). The more accurate CD approximation for the surface tension can be derived by considering two simultaneous perturbations from the reference state 0: the first involves the perturbation to a state 1 with a larger area than the reference $\mathcal{A}_1 = \mathcal{A}_0 + \Delta\mathcal{A}$ corresponding to a free-energy change of $\Delta A_{0\to1} = A_1(\mathcal{A}_1) - A_0(\mathcal{A}_0)$ as before; the second involves the symmetrical perturbation to a state -1 with a smaller area than the reference $\mathcal{A}_{-1} = \mathcal{A}_0 - \Delta\mathcal{A}$ corresponding to a free-energy change of $\Delta A_{0\to-1} = A_{-1}(\mathcal{A}_{-1})$

Downloaded 10 Oct 2005 to 155.198.160.109. Redistribution subject to AIP license or copyright, see http://jcp.aip.org/jcp/copyright.jsp

$-A_0(\mathcal{A}_0)$. The CD approximation for the surface tension can now be given as

$$\gamma = \left(\frac{\partial A}{\partial \mathcal{A}}\right)_{\mathrm{CD}} \approx \frac{A_1(\mathcal{A}_0+\Delta\mathcal{A}) - A_{-1}(\mathcal{A}_0-\Delta\mathcal{A})}{2\Delta\mathcal{A}} = \frac{\Delta A_{0\to 1} - \Delta A_{0\to -1}}{2\Delta\mathcal{A}}, \tag{64}$$

where the free-energy differences $\Delta A_{0\to 1}$ and $\Delta A_{0\to -1}$ must now be computed from the separate averages of Boltzmann factors for the corresponding change in potential energy [cf. Eq. (51)]; this can be undertaken in an efficient manner with little extra computational effort by expressing the configurational energy in terms of reduced coordinates. The use of a CD approximation not only improves the accuracy of the computed surface tension, but also allows one to circumvent the problem associated with an asymmetry in the free-energy differences which is inherent in systems of particles interacting through discontinous potentials; a more thorough investigation of this more technical aspect of the test-area method will be presented in future work.[98]

The advantage of our test-area method is that it is very simple, efficient, and can be implemented within a single simulation of an inhomogeneous system. The method is completely general and can be applied to pure systems and mixtures, including molecules which interact through discontinuous potentials or are nonspherical and complex (atomistic). In common with the other direct approaches based on the mechanical relation for the surface tension (see Sec. II A), the test-area method can be applied easily at low temperatures where finite-size scaling methods (see Sec. II C) are inappropriate; Binder's approach offers a distinct advantage if one is interested in the critical region. As we will show in Sec. III the values of the vapor-liquid surface tension of Lennard-Jones and square-well fluids computed with the test-area Monte Carlo approach are of at least the same accuracy as the most reliable data obtained with the mechanical relation.

Before concluding this section, it is important to mention that as well as being frequently used to determine the chemical potential (Widom insertion), free-energy perturbation methods have also been employed to compute the pressure without the need for the virial relation: in this case the pressure $P=-(\partial A/\partial V)_{N,T}$ can be determined from the change in the free energy for small perturbations in the volume. Eppenga and Frenkel[99] first described this type of test-volume technique in the case of hard-core particles, and the technique has now been applied to systems with continuous potentials[100] and to lattice models.[101] As far as the surface tension is concerned Singh *et al.*[47] attempted to compute γ for a square-well fluid from the corresponding pressure tensors using a test-volume perturbation technique; the accuracy of the surface tension obtained in this way turned out to be very poor, possibly because of the problem related to the asymmetry in the free-energy difference referred to earlier.

III. RESULTS AND DISCUSSION

We are now in a position to present some computations of the interfacial tension using the test-area simulation technique described in detail in Sec. II D, and make some comparisons with existing data determined using the mechanical, free-energy difference, and Landau free-energy barrier approaches. In this paper we focus on the vapor-liquid surface tension of the Lennard-Jones and square-well fluids as the vapor-liquid phase equilibrium is well characterized for these systems and there are ample simulation data for comparison. In view of the large body of literature on the surface tension of these simple fluids, only representative examples will be examined here.

All the simulations are performed with a standard Metropolis Monte Carlo (MC-*NVT*) algorithm.[21] The technique for setting up an equilibrated inhomogeneous reference system corresponding to a liquid film in coexistence with its vapor is given in Sec. II D. We now give specific details pertaining to the simulation data reported in this section. In the case of the Lennard-Jones systems, $N=1372$ particles are simulated, and slightly smaller system sizes of $N=864$ are studied for the square-well systems. The LJ systems are equilibrated for 5×10^5 Monte Carlo cycles to "relax" the liquid film while the square-well (SW) systems are equilibrated for 5×10^6 Monte Carlo cycles, where 1 cycle corresponds to N trial particle moves. The magnitude of the particle displacement is adjusted to give a $\sim$30% to 40% acceptance rate. Test-area perturbations are then performed once every cycle to compute the average Boltzmann factors of the difference in configurational energy which are required to determine the change in free energy and surface tension [cf. Eq. (60)]; for improved accuracy the central difference approximation is used to approximate the derivative of the free energy from Eq. (64) so that positive and negative perturbations in the area of the interface are performed simultaneously and two independent averages are made for the corresponding free-energy differences. Appropriate values of the relative perturbation in the surface area for the systems under investigation are $\Delta\mathcal{A}^*=\Delta\mathcal{A}/\mathcal{A}_0=\pm0.0005$ for the Lennard-Jones fluid and $\Delta\mathcal{A}^*=\pm0.0001$ for the square-well fluid. A complete analysis of the dependence of the accuracy of the surface tension on the system size and the magnitude of the perturbation in the interfacial area is given elsewhere.[98,102] For LJ systems, the averages are determined over 1×10^6 cycles and the reported errors are obtained by determining the standard deviation of the mean computed by dividing the averaging run into 10 subaverages. In the case of the SW systems with $\lambda/\sigma=1.5$ and 1.75, the averages are determined over 5×10^6 cycles divided into 20 subaverages; for SW systems with $\lambda/\sigma=1.25$, the length of the averaging run and the number of subaverages are twice as large in order to get reasonable statistics. A range of temperatures is simulated within the vapor-liquid coexistence envelope for each system; the temperature is given in reduced form $T^*=kT/\varepsilon$. The Lennard-Jones and square-well pair potentials are characterized by the diameter σ and well-depth ε parameters; an extra parameter λ defines the range of the potential for the square-well model.

Downloaded 10 Oct 2005 to 155.198.160.109. Redistribution subject to AIP license or copyright, see http://jcp.aip.org/jcp/copyright.jsp

TABLE I. The reduced surface tension $\gamma^* = \gamma\sigma^2/\varepsilon$ for the vapor-liquid interface of the Lennard-Jones system with a cutoff $r_c/\sigma = 2.5$ (unshifted) computed with the test-area Monte Carlo (TAMC) simulation method as a function of reduced temperature $T^* = kT/\varepsilon$. The systems of $N = 1372$ LJ particles are equilibrated for 5×10^5 MC cycles, and averages are accumulated over 1×10^6 cycles; 1 cycle involves N MC trial displacements. Test changes in the area of $\Delta\mathcal{A}^* = \Delta\mathcal{A}/\mathcal{A}_0 = \pm 0.0005$ are made once every cycle. The errors are estimated from the standard deviation of the mean determined from ten subaverages each of 1×10^5 cycles.

T^*	γ^*
0.650	0.891 ±0.013
0.675	0.850 ±0.005
0.700	0.779 ±0.004
0.720	0.748 ±0.016
0.750	0.684 ±0.014
0.800	0.596 ±0.010
0.850	0.506 ±0.016
0.900	0.413 ±0.011
0.950	0.323 ±0.007
1.000	0.245 ±0.008
1.050	0.168 ±0.008
1.100	0.101 ±0.012
1.100	0.095 ±0.014
1.120	0.073 ±0.011

The values of the reduced vapor-liquid surface tension $\gamma^* = \gamma\sigma^2/\varepsilon$ are reported in Tables I and II for the Lennard-Jones systems with cutoffs of $r_c/\sigma = 2.5$ and 5.5, and Tables III–V for square-well systems with ranges of $\lambda/\sigma = 1.25$, 1.5, and 1.75. The temperature dependence of the surface tension of the Lennard-Jones system with a cutoff of $r_c/\sigma = 2.5$ (unshifted) is depicted in Fig. 1. The data obtained from the test-area Monte Carlo method discussed in Sec. II D are plotted in the figure, and reported in Table I. The surface tension

TABLE II. The reduced surface tension $\gamma^* = \gamma\sigma^2/\varepsilon$ for the vapor-liquid interface of the Lennard-Jones system with a cutoff $r_c/\sigma = 5.5$ (unshifted) computed with the TAMC simulation method as a function of reduced temperature $T^* = kT/\varepsilon$. The systems of $N = 1372$ LJ particles are equilibrated for 5×10^5 MC cycles, and averages are accumulated over 1×10^6 cycles; 1 cycle involves N MC trial displacements. Test changes in the area of $\Delta\mathcal{A}^* = \Delta\mathcal{A}/\mathcal{A}_0 = \pm 0.0005$ are made once every cycle. The errors are estimated from the standard deviation of the mean determined from ten subaverages each of 1×10^5 cycles.

T^*	γ^*
0.70	1.086 ±0.023
0.72	1.046 ±0.009
0.75	0.967 ±0.018
0.80	0.870 ±0.011
0.85	0.769 ±0.016
0.90	0.654 ±0.011
0.95	0.559 ±0.006
1.00	0.456 ±0.010
1.05	0.363 ±0.007
1.10	0.276 ±0.009
1.13	0.223 ±0.011
1.15	0.188 ±0.008
1.17	0.158 ±0.011
1.20	0.116 ±0.009
1.23	0.085 ±0.008

TABLE III. The reduced surface tension $\gamma^* = \gamma\sigma^2/\varepsilon$ for the vapor-liquid interface of the square-well system with a range $\lambda/\sigma = 1.25$ computed with the TAMC simulation method as a function of reduced temperature $T^* = kT/\varepsilon$. The systems of $N = 864$ SW particles are equilibrated for 5×10^6 MC cycles, and averages are accumulated over 1×10^7 cycles; 1 cycle involves N MC trial displacements. Test changes in the area of $\Delta\mathcal{A}^* = \Delta\mathcal{A}/\mathcal{A}_0 = \pm 0.0001$ are made once every cycle. The errors are estimated from the standard deviation of the mean determined from 40 subaverages each of 2.5×10^5 cycles.

T^*	γ^*
0.61	0.396 ±0.024
0.62	0.340 ±0.021
0.63	0.319 ±0.023
0.64	0.302 ±0.024
0.65	0.275 ±0.020
0.66	0.252 ±0.023
0.67	0.246 ±0.023
0.68	0.188 ±0.021
0.686	0.181 ±0.019
0.70	0.153 ±0.014
0.71	0.116 ±0.020
0.72	0.085 ±0.015

is computed to an accuracy of between 0.5% and 4% at low and moderate temperatures, deteriorating to about 15% close to the critical point. Also shown on the figure are preliminary data also obtained with test-area perturbations, but for shorter runs.[102] The corresponding molecular-dynamics results of Trokhymchuk and Alejandre[34] determined from the tensorial components of the pressure with the mechanical relation of Kirkwood and Buff (see Sec. II A) are included in Fig. 1 for comparison; the data obtained via the mechanical route for the system of $N = 2048$ particles are seen to be of comparable accuracy to those from the test-area method. A Guggenheim[1,103] corresponding-states law

TABLE IV. The reduced surface tension $\gamma^* = \gamma\sigma^2/\varepsilon$ for the vapor-liquid interface of the square-well system with a range $\lambda/\sigma = 1.5$ computed with the TAMC simulation method as a function of reduced temperature $T^* = kT/\varepsilon$. The systems of $N = 864$ SW particles are equilibrated for 5×10^6 MC cycles, and averages are accumulated over a 5×10^6 cycles; 1 cycle involves N MC trial displacements. Test changes in the area of $\Delta\mathcal{A}^* = \Delta\mathcal{A}/\mathcal{A}_0 = \pm 0.0001$ are made once every cycle. The errors are estimated from the standard deviation of the mean determined from 20 subaverages each of 2.5×10^5 cycles.

T^*	γ^*
0.665	0.850 ±0.016
0.70	0.794 ±0.018
0.75	0.697 ±0.020
0.80	0.615 ±0.018
0.85	0.534 ±0.016
0.90	0.468 ±0.018
0.95	0.336 ±0.020
1.00	0.288 ±0.020
1.05	0.205 ±0.014
1.10	0.153 ±0.014
1.12	0.093 ±0.017
1.15	0.097 ±0.012

Downloaded 10 Oct 2005 to 155.198.160.109. Redistribution subject to AIP license or copyright, see http://jcp.aip.org/jcp/copyright.jsp

TABLE V. The reduced surface tension $\gamma^*=\gamma\sigma^2/\varepsilon$ for the vapor-liquid interface of the square-well system with a range $\lambda/\sigma=1.75$ computed with the TAMC simulation method as a function of reduced temperature $T^*=kT/\varepsilon$. The systems of $N=864$ SW particles are equilibrated for 5×10^6 MC cycles, and averages are accumulated over a further 5×10^6 cycles; 1 cycle involves N MC trial displacements. Test changes in the area of $\Delta\mathcal{A}^*=\Delta\mathcal{A}/\mathcal{A}_0=\pm0.0001$ are made once every cycle. The errors are estimated from the standard deviation of the mean determined from 20 subaverages each of 2.5×10^5 cycles.

T^*	γ^*
0.904	1.374 ±0.025
1.000	1.156 ±0.025
1.084	0.967 ±0.024
1.15	0.861 ±0.021
1.265	0.664 ±0.021
1.322	0.587 ±0.020
1.394	0.500 ±0.022
1.45	0.403 ±0.017
1.55	0.265 ±0.015
1.60	0.203 ±0.013
1.65	0.133 ±0.015
1.70	0.102 ±0.015

$$\gamma=\gamma_0(1-T/T_c)^{\mu_G} \tag{65}$$

is used to correlate the data. The optimal fit to the data is obtained with a "zero-temperature" surface tension of $\gamma_0^*=2.35\pm0.01$, using the Guggenheim mean-field critical exponent $\mu_G=11/9$, and the value of the critical temperature $T_c^*=1.189$ reported by Wilding.[104]

As was mentioned in the Introduction the surface tension of the Lennard-Jones fluid is very sensitive to the value of the cutoff that is employed, at least for $r_c/\sigma<5$. The vapor-liquid surface tension of the Lennard-Jones fluid with $r_c/\sigma=5.5$ (unshifted) obtained with the test-area Monte Carlo method is given in Table II and plotted in Fig. 2. The surface tension is seen to be almost twice that of the system with $r_c/\sigma=2.5$ at intermediate temperatures, and about 40% higher in the region of the triple point. The preliminary data[102] obtained with the test-area method for shorter runs are also shown, and are found to exhibit larger errors. As for the system with the shorter cutoff the test-area data are comparable to the data obtained by molecular dynamics with the mechanical relation.[34] The surface tension data obtained by Miyazaki *et al.*[26] and that by Salomons and Mareschal[57] determined using the free-energy difference method described in Sec. II B is plotted in Fig. 2 for comparison. The free-energy difference data are seen to be significantly less accurate than those obtained with either the mechanical or test-area methods; the point of Miyazaki *et al.* close to the triple point is seen to overestimate the surface tension, and as has been discussed in Sec. II B this could be due to the use of the surface free-energy A^s without correcting for the surface number of particles N^s. It is also interesting to assess the data obtained using the Landau free-energy barrier approach outlined in Sec. II C; as expected with this type of finite-size scaling approach the data of Hunter and Reinhardt[80] provide a good description of the near-critical region, but do not extend to lower temperatures; the accuracy of the technique decreases as the temperature is lowered as can also be seen in Fig. 2 with the data of Potoff and Panagiotopoulos.[81] By using transition matrix Monte Carlo, Errington[82] has ex-

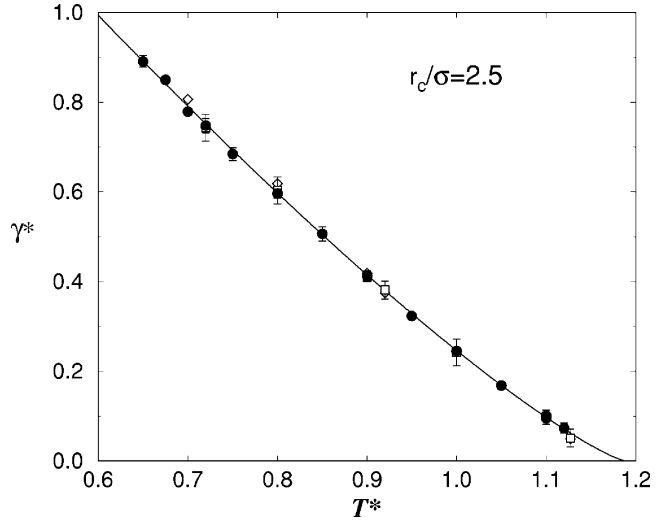

FIG. 1. Comparison of the reduced surface tension $\gamma^*=\gamma\sigma^2/\varepsilon$ for the vapor-liquid interface of the Lennard-Jones system with a cutoff $r_c/\sigma=2.5$ (unshifted) as a function of reduced temperature $T^*=kT/\varepsilon$: the black circles correspond to the simulation results obtained in this work with the TAMC technique (see Table I for details); the squares to preliminary TAMC data (Ref. 102); and the diamonds to the results of Trokhymchuk and Alejandre (Ref. 34) determined from the mechanical route. The curve represents the Guggenheim corresponding-states law [cf. Eq. (65)] with $\mu_G=11/9$, $\gamma_0^*=2.35\pm0.01$, and $T_c^*=1.189$ (Ref. 104).

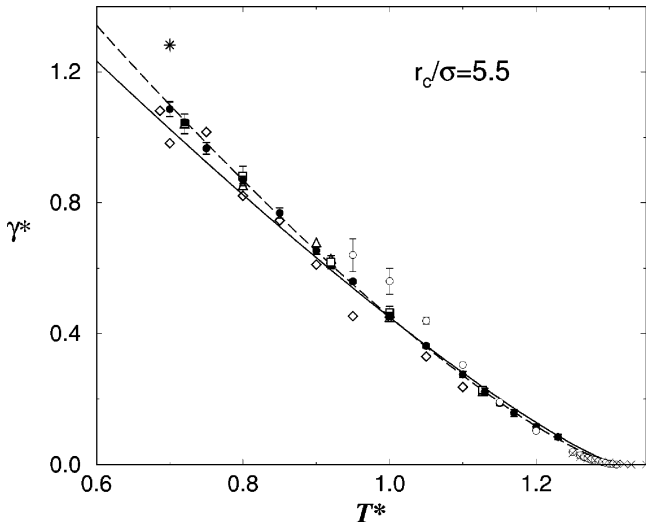

FIG. 2. Comparison of the reduced surface tension $\gamma^*=\gamma\sigma^2/\varepsilon$ for the vapor-liquid interface of the Lennard-Jones system with a cutoff $r_c/\sigma=5.5$ (unshifted) as a function of reduced temperature $T^*=kT/\varepsilon$: the black circles correspond to the simulation results obtained in this work with the TAMC technique (see Table II for details); the squares to preliminary TAMC data (Ref. 102); the triangles to the results of Trokhymchuk and Alejandre (Ref. 34) determined from the mechanical route; the asterisk to the result of Miyazaki *et al.* (Ref. 26) and the diamonds to the results of Salomons and Mareschal (Ref. 57) both obtained with the free-energy difference method of Bennett; the circles to the data of Potoff and Panagiotopoulos (Ref. 81), and the crosses to that of Hunter and Reinhardt (Ref. 80), both obtained using a finite-size scaling technique. The continuous curve represents the Guggenheim corresponding-states law [cf. Eq. (65)] with $\mu_G=11/9$, $\gamma_0^*=2.60\pm0.04$, and $T_c^*=1.312$ (Ref. 105). The dashed curve corresponds to the unconstrained correlation to the data with $\mu_G=1.30\pm0.01$ and $\gamma_0^*=2.94\pm0.05$.

Downloaded 10 Oct 2005 to 155.198.160.109. Redistribution subject to AIP license or copyright, see http://jcp.aip.org/jcp/copyright.jsp

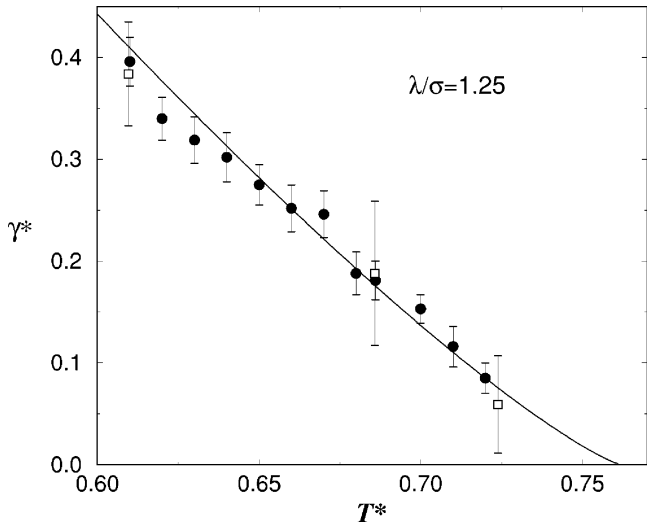

FIG. 3. Comparison of the reduced surface tension $\gamma^*=\gamma\sigma^2/\varepsilon$ for the vapor-liquid interface of the square-well system with a range of $\lambda/\sigma=1.25$ as a function of reduced temperature $T^*=kT/\varepsilon$: the black circles correspond to the simulation results obtained in this work with the TAMC technique (see Table III for details); and the squares to preliminary TAMC data (Refs. 16 and 102). The curve represents the Guggenheim corresponding-states law [cf. Eq. (65)] with $\mu_G=11/9$, $\gamma_0^*=2.49\pm0.06$, and $T_c^*=0.762$ (Ref. 106).

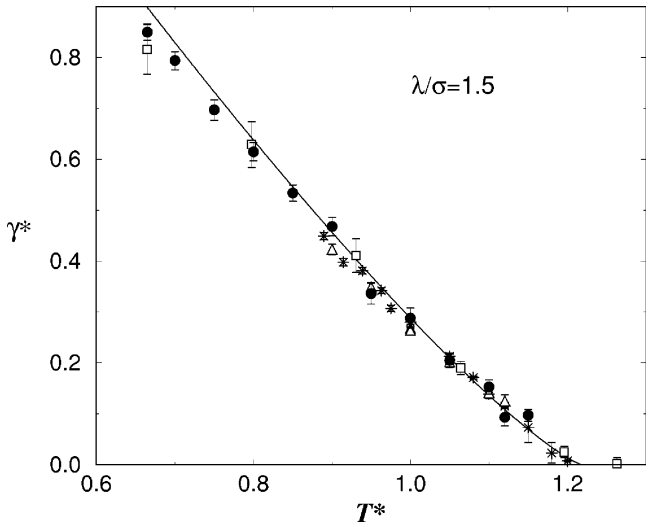

FIG. 4. Comparison of the reduced surface tension $\gamma^*=\gamma\sigma^2/\varepsilon$ for the vapor-liquid interface of the square-well system with a range of $\lambda/\sigma=1.5$ as a function of reduced temperature $T^*=kT/\varepsilon$: the black circles correspond to the simulation results obtained in this work with the TAMC technique (see Table IV for details); the squares to preliminary TAMC data (Refs. 16 and 102); the triangles to the results of Orea *et al.* (Ref. 45) from the mechanical route; and the asterisks to the data obtained by Singh *et al.* (Ref. 47) with a finite-size scaling approach. The curve represents the Guggenheim corresponding-states law [cf. Eq. (65)] with $\mu_G=11/9$, $\gamma_0^*=2.36\pm0.08$, and $T_c^*=1.218$ (Ref. 106).

tended the use of the finite-size scaling method to much lower temperatures, but as we shall see later this approach does not appear to work as well for the square-well model. The Guggenheim corresponding-states correlations [cf. Eq. (65)] are also depicted in Fig. 2, where we have taken the value of the critical temperature $T_c^*=1.312$ of Potoff and Panagiotopoulos.[105] In the case of the system with $r_c/\sigma=5.5$ the use of the Guggenheim critical exponent $\mu_G=11/9$ and the best-fit value of $\gamma_0^*=2.60\pm0.04$ does not appear to provide a good representation of the data, particularly at lower temperatures; an unconstrained correlation of both parameters yields optimal values of $\mu_G=1.30\pm0.01$ and $\gamma_0^*=2.94\pm0.05$. This is rather surprising as the Guggenheim mean-field correlation describes the data for the $r_c/\sigma=2.5$ system accurately, and it can also be used for the square-well systems.

We now turn to the simulation of the vapor-liquid surface tension of the square-well fluid, which as we have discussed earlier is more difficult to compute from a mechanical route because of the discontinuous nature of the potential. The data for the square-well system with $\lambda/\sigma=1.25$, 1.5, and 1.75 are collected in Tables III–V. The accuracy of the test-area method is most severely tested for the system with the shortest intermolecular potential range ($\lambda/\sigma=1.25$), where the surface tension is computed with an accuracy of 6% to 17%. The temperature dependence of the square-well system with $\lambda/\sigma=1.25$ is shown in Fig. 3, and a degree of scatter is apparent. Also shown on the figure are some preliminary data[16,102] obtained with the test-area method which, though consistent with our current data, are seen to exhibit larger error bars. In the case of simulations of square-well fluids the central difference approximation Eq. (64) has to be used to provide accurate estimates for the surface tension; this appears to be related to the asymmetry of the free-energy change in such systems[102] and is the subject of current work.[98] The Guggenheim mean-field correlation of the data with $\mu_G=11/9$ and $\gamma_0^*=2.49\pm0.06$, and a critical temperature of $T_c^*=0.762$ (Ref. 106) is also included in Fig. 3 and is seen to adequately describe the data.

There are more published data for the surface tension of the commonly studied square-well system with $\lambda/\sigma=1.5$. The surface-tension data obtained with our test-area Monte Carlo approach are compared with the data obtained by Orea *et al.*[45] with the mechanical route using a special method to estimate the tensorial components of the pressure, and with those obtained by Singh *et al.*[47] with the finite-size scaling approach using a transition matrix Monte Carlo technique to sample the lower temperatures; some preliminary calculations with the test-area method are also included.[16,102] As can be seen from Fig. 4, the values of the surface tension obtained with the three methods are found to be in agreement. The data of Singh *et al.* (and those of Orea *et al.* for that matter) do not extend to temperatures lower than about $T^*=0.9$, though it is not clear if this is due to the inherent problem with the finite-size scaling technique. As for the system with $\lambda/\sigma=1.25$, the Guggenheim mean-field correlation with $\mu_G=11/9$ and $\gamma_0^*=2.36\pm0.08$, and a critical temperature of $T_c^*=1.218$ (Ref. 106) provides a good representation of the data.

We end our assessment of our method by reporting our computations of the surface tension of the square-well system with $\lambda/\sigma=1.75$. Our current values of the surface tension and the preliminary estimates with the test-area method[16,102] are compared with the finite-size scaling data of Singh *et al.*[47] in Fig. 5. Again the data obtained with the test-area and finite-size scaling techniques appear to be of comparable accuracy, though the latter does not extend to the lowest temperatures. In this case the Guggenheim mean-field

Downloaded 10 Oct 2005 to 155.198.160.109. Redistribution subject to AIP license or copyright, see http://jcp.aip.org/jcp/copyright.jsp

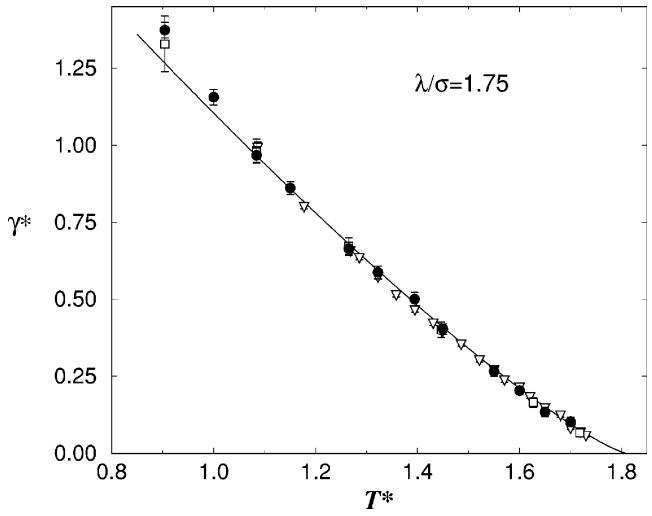

FIG. 5. Comparison of the reduced surface tension $\gamma^*=\gamma\sigma^2/\varepsilon$ for the vapor-liquid interface of the square-well system with a range of $\lambda/\sigma=1.75$ as a function of reduced temperature $T^*=kT/\varepsilon$: the black circles correspond to the simulation results obtained in this work with the TAMC technique (see Table V for details); the squares to preliminary TAMC data (Refs. 16 and 102); and the triangles to the data obtained by Singh *et al.* (Ref. 47) from a finite-size scaling technique. The curve represents the Guggenheim corresponding-states law [cf. Eq. (65)] with $\mu_G=11/9$, $\gamma_0^*=2.60\pm0.04$, and $T_c^*=1.808$ (Ref. 106).

correlation corresponds to $\mu_G=11/9$ and $\gamma_0^*=2.60\pm0.04$, with a critical temperature of $T_c^*=1.808$ (Ref. 106).

IV. CONCLUSION

A new technique is described for the computation of the surface tension from a single simulation. The method is based on the evaluation of the change in the free energy due to a test-area (TA) perturbation, and can easily be implemented within either Monte Carlo (TAMC) or molecular-dynamics (TAMD) simulations. The test-area approach is completely general and can be applied to different types of interfaces (vapor-liquid, liquid-liquid, fluid-solid, etc.) of pure systems and mixtures consisting of complex polyatomic molecules. A key advantage is that as it is a thermodynamic approach one does not have the problems associated with the calculation of the tensorial components of the pressure that are required for a mechanical evaluation of the surface tension. This is particularly relevant in the case of systems interacting through discontinous potentials or nonspherical molecules. The adequacy of the test-area approach for the vapor-liquid surface tension has been assessed by comparisons with existing data from mechanical, free-energy difference, and finite-size scaling methods. The TAMC data compare favorably with the most accurate evaluations available for the Lennard-Jones and square-well systems. The method is currently being applied to systems of nonspherical molecules and mixtures. As an indication of the accuracy of the test-area method for nonspherical molecules we present preliminary data for the vapor-liquid surface tension of the Gay-Berne model (anisotropic version of the Lennard-Jones potential): the surface-tension data for the Gay-Berne system with model parameters $\kappa=3$ and $\kappa'=1$ for temperatures $T^*=0.60$ (which corresponds to vapor-nematic coexistence) and 0.65 (which corresponds to vapor-isotropic coexistence) obtained with the TAMC approach ($\gamma^*=0.331\pm0.018$ and 0.212 ± 0.016, respectively) are in good agreement with the published values obtained from the mechanical relation ($\gamma^*=0.35\pm0.08$ and 0.24 ± 0.04, respectively).[9] In the case of Gay-Berne systems, the TAMC method is seen to provide a significantly improved accuracy for the surface tension. This is certainly a testament to the generality of the test-area technique for the simulation of the surface tension in more complex systems.

ACKNOWLEDGMENTS

We are grateful to Erich Müller, Jean-Pierre Hansen, and Ruth Lynden-Bell for useful discussions. One of the authors (G.J.G.) would like to thank BP Exploration for funding a studentship. We acknowledge further support from the EPSRC of the UK (GR/N03358, GR/N35991, and GR/R09497), the Joint Research Equipment Initiative (JREI) for computer hardware (GR/M94427), and the Royal Society-Wolfson Foundation for the award of a refurbishment grant. Two of the authors (F.J.B. and E.dM.) are also grateful for financial support from Project No. FIS2004-06227-C02-01 of the Spanish Dirección General de Investigación. One of the authors (E.dM.) also acknowledges financial support from Secretaría de Estado de Educación y Universidades (Spain) within the Programa de Movilidad de Profesorado.

[1] J. S. Rowlinson and B. Widom, *Molecular Theory of Capillarity* (Clarendon, Oxford, 1982).
[2] D. Henderson, *Fundamentals of Inhomogeneous Fluids* (Dekker, New York, 1992).
[3] H. T. Davis, *Statistical Mechanics of Phases, Interfaces, and Thin Films* (VCH, Weinheim, 1996).
[4] J. D. van der Waals, Z. Phys. Chem. **13**, 657 (1894); English translation, J. S. Rowlinson, J. Stat. Phys.20, 197 (1979).
[5] D. Nicholson and N. G. Parsonage, *Computer Simulation and the Statistical Mechanics of Adsorption* (Academic, London, 1982).
[6] J. C. Shelley and M. Y. Shelley, Curr. Opin. Colloid Interface Sci. **5**, 101 (2000).
[7] D. J. Tobias, K. C. Tu, and M. L. Klein, Curr. Opin. Colloid Interface Sci. **2**, 15 (1997).
[8] L. Saiz and M. L. Klein, Acc. Chem. Res. **35**, 482 (2002).
[9] E. Martín del Río and E. de Miguel, Phys. Rev. E **55**, 2916 (1997).
[10] M. Bates and C. Zannoni, Chem. Phys. Lett. **280**, 40 (1997).
[11] S. J. Mills, C. M. Care, M. P. Neal, and D. J. Cleaver, Phys. Rev. E **58**, 3284 (1998).
[12] E. de Miguel and E. Martín del Río, Int. J. Mod. Phys. C **10**, 431 (1999).
[13] N. Akino, F. Schmid, and M. P. Allen, Phys. Rev. E **63**, 041706 (2001).
[14] A. Galindo, A. J. Haslam, S. Varga, G. Jackson, A. Vanakaras, D. J. Photinos, and D. A. Dunmur, J. Chem. Phys. **119**, 5216 (2003).
[15] J. Winkelmann, J. Phys.: Condens. Matter **13**, 4739 (2001).
[16] G. J. Gloor, G. Jackson, F. J. Blas, E. Martín del Río, and E. de Miguel, J. Chem. Phys. **121**, 12740 (2004).
[17] J. G. Kirkwood and F. P. Buff, J. Chem. Phys. **17**, 338 (1949).
[18] C. H. Bennett, J. Comput. Phys. **22**, 245 (1976).
[19] K. Binder, Phys. Rev. A **25**, 1699 (1982).
[20] F. P. Buff, R. A. Lovett, and F. H. Stillinger Jr., Phys. Rev. Lett. **15**, 621 (1965).
[21] M. P. Allen and D. J. Tildesley, *Computer Simulation of Liquids* (Clarendon, Oxford, 1987).
[22] C. A. Croxton and R. P. Ferrier, J. Phys. C **4**, 2447 (1971).
[23] H. J. Leamy, G. H. Gilmer, K. A. Jackson, and P. Bennema, Phys. Rev. Lett. **30**, 601 (1973).
[24] J. K. Lee, J. A. Barker, and G. M. Pound, J. Chem. Phys. **60**, 1976 (1974).
[25] K. S. Liu, J. Chem. Phys. **60**, 4226 (1974).

Downloaded 10 Oct 2005 to 155.198.160.109. Redistribution subject to AIP license or copyright, see http://jcp.aip.org/jcp/copyright.jsp

[26] J. Miyazaki, J. A. Barker, and G. M. Pound, J. Chem. Phys. **64**, 3364 (1976).
[27] A. C. L. Opitz, Phys. Lett. A **47**, 439 (1974).
[28] F. F. Abraham, D. E. Schreiber, and J. A. Barker, J. Chem. Phys. **62**, 1958 (1975).
[29] G. A. Chapela, G. Saville, and J. S. Rowlinson, Faraday Discuss. Chem. Soc. **59**, 22 (1975).
[30] M. Rao and D. Levesque, J. Chem. Phys. **65**, 3233 (1976).
[31] G. A. Chapela, G. Saville, S. M. Thompson, and J. S. Rowlinson, J. Chem. Soc., Faraday Trans. 2 **73**, 1133 (1977).
[32] L.-J. Chen, J. Chem. Phys. **103**, 10214 (1995).
[33] C. D. Holcomb, P. Clancy, and J. A. Zollweg, Mol. Phys. **78**, 437 (1993).
[34] A. Trokhymchuk and J. Alejandre, J. Chem. Phys. **111**, 8510 (1999).
[35] M. Matsumoto and Y. Kataoka, J. Chem. Phys. **88**, 3233 (1988).
[36] J. Alejandre, D. J. Tildesley, and G. A. Chapela, J. Chem. Phys. **102**, 4574 (1995).
[37] T.-M. Chang, K. A. Peterson, and L. X. Dang, J. Chem. Phys. **103**, 7502 (1995).
[38] Y. L. Yea, C. Zhang, H. Held, A. M. Mebel, X. Wei, S. H. Lin, and Y. R. Shen, J. Chem. Phys. **114**, 1837 (2001).
[39] F. Goujon, P. Malfreyt, A. Boutin, and A. H. Fuchs, J. Chem. Phys. **116**, 8106 (2002).
[40] J. P. Nicolas and B. Smit, Mol. Phys. **100**, 2471 (2002).
[41] P. Smith, R. M. Lynden-Bell, J. C. Earnshaw, and W. Smith, Mol. Phys. **96**, 249 (1999).
[42] J. G. Harris, J. Phys. Chem. **96**, 5077 (1992).
[43] I. Benjamin, Annu. Rev. Phys. Chem. **48**, 407 (1997).
[44] J. R. Henderson and F. van Swol, Mol. Phys. **56**, 1313 (1985).
[45] P. Orea, Y. Duda, and J. Alejandre, J. Chem. Phys. **118**, 5635 (2003).
[46] P. Orea, Y. Duda, V. C. Weiss, W. Schröer, and J. Alejandre, J. Chem. Phys. **120**, 11754 (2004).
[47] J. K. Singh, D. A. Kofke, and J. R. Errington, J. Chem. Phys. **119**, 3405 (2003).
[48] J. H. Irving and J. G. Kirkwood, J. Chem. Phys. **18**, 817 (1950).
[49] P. Schofield and J. R. Henderson, Proc. R. Soc. London, Ser. A **379**, 231 (1982).
[50] J.-P. Hansen and I. R. McDonald, *Theory of Simple Liquids*, 2nd ed. (Academic, London, 1986).
[51] A. Harasima, J. Phys. Soc. Jpn. **8**, 343 (1953).
[52] J. P. R. B. Walton, D. J. Tildesley, J. S. Rowlinson, and J. R. Henderson, Mol. Phys. **48**, 1357 (1983).
[53] N. N. Bogoliubov, J. Phys. (USSR) **10**, 256, 265 (1946).
[54] H. S. Green, Proc. R. Soc. London, Ser. A **189**, 103 (1947).
[55] F. P. Buff, Z. Elektrochem. **56**, 311 (1952).
[56] A. G. McLellan, Proc. R. Soc. London, Ser. A **213**, 274 (1952); *ibid.* **217**, 92 (1953).
[57] E. Salomons and M. Mareschal, J. Phys.: Condens. Matter **3**, 3645 (1991).
[58] D. Duque and L. F. Vega, J. Chem. Phys. **121**, 8611 (2004).
[59] D. A. Kofke and P. T. Cummings, Mol. Phys. **92**, 973 (1997).
[60] D. A. Kofke and P. T. Cummings, Fluid Phase Equilib. **150**, 41 (1998).
[61] M. P. Moody and P. Attard, J. Chem. Phys. **120**, 1892 (2004).
[62] K. K. Mon and D. Jasnow, Phys. Rev. A **30**, 670 (1984).
[63] K. K. Mon and D. Jasnow, Phys. Rev. A **31**, 4008 (1985).
[64] J. Potvin and C. Rebbi, Phys. Rev. Lett. **62**, 3062 (1989).
[65] H. Gausterer, J. Potvin, C. Rebbi, and S. Sanielevici, Physica A **192**, 525 (1993).
[66] J. E. Hunter III, W. P. Reinhardt, and T. F. Davis, J. Chem. Phys. **99**, 6856 (1993).
[67] M. Hasenbusch, J. Phys. I (France) **3**, 753 (1993).
[68] L. D. Landau and E. M. Lifshitz, *Statistical Physics*, 3rd ed. (Pergamon, London, 1980).
[69] R. M. Lynden-Bell, Mol. Phys. **86**, 1353 (1995).
[70] B. A. Berg and T. Neuhaus, Phys. Rev. Lett. **68**, 9 (1992).
[71] W. Janke, B. A. Berg, and M. Katoot, Nucl. Phys. B **382**, 649 (1992).
[72] B. A. Berg, U. Hansmann, and T. Neuhaus, Phys. Rev. B **47**, 497 (1993).
[73] B. A. Berg, U. Hansmann, and T. Neuhaus, Z. Phys. B: Condens. Matter **90**, 229 (1993).
[74] A. Billoire, T. Neuhaus, and B. A. Berg, Nucl. Phys. B **413**, 795 (1994).
[75] T. S. Jain and J. J. de Pablo, J. Chem. Phys. **118**, 4226 (2003).
[76] J. S. van Duijneveldt and D. Frenkel, J. Chem. Phys. **96**, 4655 (1992).
[77] R. M. Lynden-Bell, J. S. van Duijneveldt, and D. Frenkel, Mol. Phys. **80**, 801 (1993).
[78] R. Allen, S. Melchionna, and J.-P. Hansen, Phys. Rev. Lett. **89**, 175502 (2002).
[79] R. Allen, S. Melchionna, and J.-P. Hansen, J. Chem. Phys. **119**, 3905 (2003).
[80] J. E. Hunter III and W. P. Reinhardt, J. Chem. Phys. **103**, 8627 (1995).
[81] J. J. Potoff and A. Z. Panagiotopoulos, J. Chem. Phys. **112**, 6411 (2000).
[82] J. R. Errington, Phys. Rev. E **67**, 012102 (2003).
[83] J. Y. Lee and J. M. Kosterlitz, Phys. Rev. Lett. **65**, 137 (1990).
[84] G. M. Torrie and J. -P. Valleau, Chem. Phys. Lett. **28**, 578 (1974).
[85] J. D. Weeks, J. Chem. Phys. **67**, 3106 (1977).
[86] D. Bedeaux and J. D. Weeks, J. Chem. Phys. **82**, 972 (1985).
[87] M. P. Gelfand, and M. E. Fisher, Physica A **166**, 1 (1990).
[88] B. Widom, J. Chem. Phys. **39**, 2808 (1963).
[89] H. C. Longuet-Higgins, Proc. R. Soc. London, Ser. A **205**, 247 (1951).
[90] J. A. Barker, J. Chem. Phys. **19**, 1430 (1951).
[91] J. A. Barker, Proc. R. Soc. London, Ser. A **219**, 367 (1953).
[92] J. A. Pople, Proc. R. Soc. London, Ser. A **215**, 67 (1952).
[93] J. A. Pople, Proc. R. Soc. London, Ser. A **221**, 498 (1954).
[94] R. W. Zwanzig, J. Chem. Phys. **22**, 1420 (1954).
[95] J. L. Jackson and L. S. Klein, Phys. Fluids **7**, 228 (1964).
[96] E. Byckling, Physica (Amsterdam) **27**, 1030 (1961).
[97] *Handbook of Mathematical Functions with Formulas, Graphs, and Mathematical Tables*, 9th ed., edited by M. Abramowitz and I. A. Stegun (Dover, New York, 1972), pp. 877–878.
[98] E. de Miguel and G. Jackson (unpublished).
[99] R. Eppenga and D. Frenkel, Mol. Phys. **52**, 1303 (1984).
[100] V. I. Harismiadis, J. Vorholz, and A. Z. Panagiotopoulos, J. Chem. Phys. **105**, 8469 (1996).
[101] A. Provota, V. D. Prassas, and D. N. Theodorou, J. Chem. Phys. **107**, 5125 (1997).
[102] G. J. Gloor, Ph.D. thesis, Imperial College London, 2003.
[103] E. A. Guggenheim, J. Chem. Phys. **13**, 253 (1945).
[104] N. B. Wilding, Phys. Rev. E **52**, 602 (1995).
[105] J. J. Potoff and A. Z. Panagiotopoulos, J. Chem. Phys. **109**, 10914 (1998).
[106] F. del Río, E. Ávalos, R. Espíndola, L. F. Rull, G. Jackson, and S. Lago, Mol. Phys. **100**, 2531 (2002).

Downloaded 10 Oct 2005 to 155.198.160.109. Redistribution subject to AIP license or copyright, see http://jcp.aip.org/jcp/copyright.jsp